Two-phase Modeling of DDT in Granular Materials: A Critical Examination of Modeling Issues

J. B. Bdzil*, R. Menikoff, S. F. Son
Los Alamos National Laboratory

A. K. Kapila
Rensselaer Polytechnic Institute

D. S. Stewart
University of Illinois at Urbana-Champaign

March 13, 1999

Abstract

The two-phase mixture model developed by Baer and Nunziato (BN) to study the deflagration-to-detonation transition (DDT) in granular explosives is critically reviewed. The continuum-mixture theory foundation of the model is examined, with particular attention paid to the manner in which its constitutive functions are formulated. Connections between the mechanical and energetic phenomena occurring at the scales of the grains, and their manifestations on the continuum, averaged scale, are explored. The nature and extent of approximations inherent in formulating the constitutive terms, and their domain of applicability, are clarified. Deficiencies and inconsistencies in the derivation are cited, and improvements suggested. It is emphasized that the entropy inequality constrains but does not uniquely determine the phase interaction terms. The resulting flexibility is exploited to suggest improved forms for the phase interactions. These improved forms better treat the energy associated with the dynamic compaction of the bed and the single-phase limits of the model. Companion papers of this study [1, 2, 3] examine simpler, reduced models, in which the fine scales of velocity and pressure disequilibrium between the phases allow the corresponding relaxation zones to be treated as discontinuities that need not be resolved in a numerical computation.

PACS: 47.55.Kf, 47.40.-x, 05.70.L

*Corresponding author. Email: jbb@lanl.gov

1 Introduction

This paper is the first in a sequence of articles on the modeling, analysis and numerical simulation of deflagration to detonation transition (DDT) in porous energetic materials. It represents a group effort of the authors to critically evaluate and carefully reformulate two-phase continuum models that might have an extended, physically-based predictive capability for DDT. The impetus for the larger study, which includes experiments and numerical implementation of models in engineering design codes, stems from a program based at the Los Alamos National Laboratory (LANL) and aimed at the development of advanced models to assess hazards associated with the accidental initiation of detonation in a damaged explosive device. When damage causes the explosive to become cracked or pulverized, then it is more susceptible to accidental initiation of violent reaction and detonation.

This study focuses on various modeling issues that arise in the construction of a two-phase theory of DDT. To be sure, several attempts aimed at the development of such a theory exist in the DDT literature, and we shall refer to some of these in due course. We emphasize, however, that this paper is not an encyclopedic survey, nor even a retrospective, of the field. Rather, we concentrate on what may be viewed as the current state of the art, and examine it critically, with regard to its theoretical foundations (especially the manner in which principles of continuum mechanics and thermodynamics are employed in its development), the appropriateness of the modeling assumptions vis-a-vis the physical system at hand, and the way in which experimental information is incorporated into the theory. Such an examination is warranted, and indeed essential, in a problem of such complexity, so that any weaknesses, inconsistencies and deficiencies that may exist are clearly identified. For example, while it is widely recognized that thermodynamics constrains the development of a constitutive theory, the precise extent of the constraint, and more importantly, the degree of flexibility that it permits, appear not to have been fully appreciated or exploited by the currently available theories. This paper addresses, explores and clarifies the issue. It also identifies other sources of constraint, such as the requirement that a two-phase description must have an appropriate single-phase limit, and that in partitioning the dissipation between the phases one must not lose sight of this fact. The mechanics and energetics of the process of compaction are examined, with an eye on the extent and accuracy to which these aspects of the process are included in the theory. This is an important modeling issue since a proposed theory must not only predict the correct structure

of compaction waves but also the correct distribution of compaction energy. After all, it is the compaction energy that is responsible for the process of ignition.

Even though the ultimate, practical goal is the prediction of DDT in damaged materials, this study concentrates on the behavior of simpler, well-characterizable explosives, *i.e.*, granular materials with well-controlled grain sizes. Two reasons lie behind this narrower focus. First, reliable experimental information on DDT in granular materials is at hand. Second (and more important), it is crucial that the behavior of simpler explosives be thoroughly understood, and predictive models for them developed, before further complexities associated with defining the amount and nature of accidental damage are inserted into the theory.

The experimental information to which we have just referred comes from the so-called DDT-tube tests [4], [5], wherein a bed of granular explosive, such as 30% porous HMX, is subjected to a low-velocity (approximately 100 m/s) impact. Observations show that detonation does not occur immediately upon impact, but rather, is the culmination of a succession of distinct events [5], [6], [7]. Dominant identifiable features include (i) a lead compaction wave, (ii) a burn front, (iii) a high-density region called a plug, (iv) a secondary compaction wave, (v) a shock, and finally, (vi) a detonation front. Experiments [8] further reveal that (i) length scales for such processes as compaction, energy release and heat transfer can be of the order of the grain size, (ii) the overall scale of the experiment is large compared to the grain size, and (iii) the most precise, high-resolution measurements [9] of such quantities as pressure and particle velocity, representing transverse "averages" over 10 to 100 grains, are very reproducible. The implication is that the granular explosive is well-behaved, in the sense that its average response is insensitive to variations in the granular microstructure that must occur from one experiment to the next. This argues for a "continuum" hydrodynamic model of DDT in granular explosives, which manages to average out granularity and its fine-scale effects on the flow. A mathematical description at the level of the grains, even if it were feasible, would be an expensive overkill.

Within the continuum context itself there exist further options. There is the minimalist approach reflected in the recent work of Stewart *et al.* [10], where the explosive is treated essentially as a single-phase material governed by the Euler equations of hydrodynamics, with porosity and reaction progress introduced as independent thermodynamic variables. These added state variables obey new evolution equations along appropriate Lagrangian

paths. With adequate calibration this approach can reproduce the observed primary and secondary compaction wave, plug, and shock-formation behavior seen in the tube test. But if such approaches are to have wider application to a broad class of experiments beyond the DDT-tube experiment, additional complexity in the form of (i) enhanced constitutive theory and (ii) added state variables would need to be included.

We opt for a two-phase framework, for which there are several motivating factors. First, while the single-phase, minimalist description offers a simpler modeling structure, it has insufficient degrees of freedom to describe the dynamic effects of temperature, pressure and velocity disequilibrium. The structure of two-phase models is better able to deal with such issues, accepting at the same time the only data that are available for the material response functions, namely, those for the solid and gas phases in isolation. The porosity variable also enters naturally in such a description. Second, two-phase models of DDT have an extensive literature (see below) and represent a substantial investment, so that a careful consideration of both (i) the applicability of such models and (ii) the consequences resulting from their mathematical structure is merited. Third, two-phase models encompass a great variety of complex wave phenomena. Therefore, such a description (possibly with additional variables to better model energy localization, dissipation and their effect on the chemical reactions) can be regarded as a superset from which to rationally derive reduced models with fewer phenomena admitted. Viewed in this way, there is a connection to reduced models which corresponds to some enhanced understanding of the physics.

The most common two-phase treatment of the explosive as a mixture is explicitly formulated in terms of variables for its two separate constituents: a granular solid phase and a separate, combustion product gas phase. For a particularly lucid discussion of this topic see the article entitled "A Theory of Multiphase Mixtures" by Passman, Nunziato and Walsh which is Sec.(5C.6) of Appendix 5C in a monograph by Truesdell [11]. An application of this class of theories to granular explosives is exemplified by the work of Baer and Nunziato [12]; see also the contemporaneous studies of Butler and Krier [13] and Butler [14], the earlier work of Gokhale and Krier [15], and the more recent papers of Powers, Stewart and Krier [16], [17]. Bibliographies of these papers provide a wealth of additional references.

In such an approach, each phase is identifiable and the mixture assumed immiscible. The principle of phase separation is invoked. Each phase is separately assumed to be in local thermodynamic equilibrium and described by a density, specific internal energy and velocity. The phases are not,

however, in equilibrium with each other. The volume fraction of each phase is an additional variable required to specify the state of the mixture. The gas volume fraction is referred to as the porosity. Each phase is characterized by a separate equation of state (EOS). To account for the configuration-dependent energy of the granular solid, the EOS of the solid phase depends on the volume fraction as well as its density and energy. The dynamics is determined by a system of partial differential equations (PDEs). Each phase separately satisfies conservation of mass, momentum and energy. The non-equilibrium interactions between the phases are described by source terms for the exchange of mass, momentum and energy between the phases.

The evolution of the volume fraction variable requires that an additional equation be specified to affect closure of the system. For a system in which both phases are compressible, Passman, Nunziato and Walsh introduced a model where closure is achieved with a PDE for the volume fraction. They envision a thin, interfacial region, deemed to have a microinertia and a viscosity, that controls the evolution of the volume fraction. This equation is an attempt to model the way in which the microstructural forces at the interfaces act to drive the volume fraction towards equilibrium [18]. Thus, phenomena associated with the discrete, granular nature of the mixture are accounted for by the EOS of the granular phase, by the form of the volume fraction equation, and by the nature of the source terms therein. The dynamical behavior of a granular solid can be very different from that of the full-density solid phase.

Derivations of the interaction source terms in the context of explosives (and indeed, for multicomponent flows in general) are usually phenomenological and heuristic. A common practice is to postulate functional forms based on observations and experience with simpler problems. The fundamental tenets of continuum theory provide some constraints on the functional forms. Alternatively, guidance can be sought from an averaging approach [19], wherein the source terms have a form relating them to exact solutions of the microscale equations of motion. For a two-phase mixture of a granular solid and a gas, three types of source terms arise. These correspond to (i) interactions at grain-grain boundaries, (ii) interactions at interphase boundaries, and (iii) fluctuations within each phase [19]. An example of the first class is the configuration pressure, an average of the localized stress at the contacts between grains resulting from material strength. The second class is exemplified by the energy exchange due to heat transfer between the phases. Drag on the gas phase, caused by particle-velocity fluctuations during the tortuous motion of the gas through the granular bed, is an example

of the third class.

Computing power is reaching the point at which micromechanical computations can be performed and the modeling approximation tested with numerical experiments; see for example, simulation of shock compaction in copper powder by Benson [20]. While serious questions remain concerning numerical resolution and the adequacy of material models that are used, this development renders the averaging approach for developing continuum theory more attractive than it has been heretofore.

Regardless of the approach, specification of the interphase interactions remains the essence of multiphase continuum modeling. Where the various models differ most, one from the other, is in their closure assumptions and source terms. The DDT application presents a special challenge because experimental information is seldom available over a sufficiently broad range. As a result, approximations and extrapolations abound. An example is the configuration pressure, typically calibrated to quasistatic experiments but applied to predict dynamical features such as the state behind a compaction wave. Another example is the assumption that the configuration pressure β_s is a function only of the volume fraction ϕ_s, notwithstanding the fact that above its yield strength the solid flows and therefore cannot support a configuration pressure. Both are examples of approximations that, although simplistic, are forgiving; the first because the stiff EOS of the solid renders the gross mechanical features of compaction waves insensitive to the approximation, and the second because where β_s is inaccurate it is dominated by the bulk pressure in the solid, *i.e.* $\beta_s/P_s << 1$. In other cases, simplistic approximations lead to difficulties. We show, for example, that in the limit as the gas mass fraction goes to zero, insufficient attention to detail in the construction of the exchange terms can have the gas play too significant a role in the energetics of the dominant solid phase. A primary aim of this effort is to clearly articulate the modeling issues in the DDT application, and in particular, to clarify the nature of assumptions and approximations, and where feasible, their consequences through an analysis of the model.

For the purpose of this paper we take the Baer-Nunziato (BN) model as a starting point [12]. It aims at describing a granular explosive in which a gas phase fills the interstitial pores between chemically reacting solid grains. It is based directly on the previously-cited work of Passman, Nunziato and Walsh [11] on granular, multiphase mixtures. The velocity, temperature and pressure of the two phases are allowed to be unequal. A dissipation inequality for the mixture is employed to formulate the source terms, requiring that at each point the mixture entropy be nondecreasing with time. A drag

source in the momentum equations equilibrates velocities, a heat-transfer term in the energy equations equilibrates temperatures, and a relaxation equation for the volume fraction serves to equilibrate pressures. The time rate of change of volume fraction is associated with the advection of the solid phase, in keeping with BN's association of granularity with the solid phase. Due to the low pressure material strength of the grains, modeled by the configuration pressure, the solid and gas pressures are offset by β_s at equilibrium.

In contrast to the BN-model, many conventional two-phase fluid models assume pressure equilibrium. The volume fraction is then determined by an algebraic equation rather than an evolution equation. In some situations, the constraint on the volume fraction causes the PDEs for the pressure equilibrium models to become elliptic and ill posed, in the sense that the PDEs are not evolutionary, *i.e.*, with arbitrary initial data the solution is not determined for all time. The assumption of a dynamical compaction law in the BN-model, on the other hand, yields a system of hyperbolic PDEs. These PDEs have a well-defined wave structure, with one pair of acoustic modes for each phase [21]. A shock in a single phase leads to a pressure imbalance behind the shock front. At low pressures where reactivity is unimportant, the source term in the compaction equation provides a relaxation mechanism to equilibrate the pressures. When the magnitude of the compaction source term is large, a compressive wave approaches pressure equilibrium within a narrow zone and the state behind the fully or partly dispersed wave rather than the single phase shock is of physical interest.

A critical and detailed examination of the BN model reveals certain deficiencies and inconsistencies. For example, the forms adopted for the interphase source terms rely heavily on the dissipation inequality for reactive, two-phase mixtures. The BN source terms are only one realization of the many possibilities that are compatible with the dissipation inequality, and the BN derivation appears not to recognize this nonuniqueness. A part of the nonuniqueness involves the distribution of energy or entropy production between the phases for each dissipative process. We use this nonuniqueness to advantage and show that it can be used to correct inconsistencies and make improved modeling choices in the original BN model related to compaction work and to the single phase limit (porosity approaching 0 or 1).

Additionally, as Powers *et al.* [16] have noted previously, the BN model does not treat in a thermodynamically consistent manner the assumed volume-fraction dependence of the solid free energy in the development of the solid

internal energy and/or entropy production. That is, the assumed form for the differential of the solid entropy,

$$T_s d\eta_s = de_s - \frac{P_s}{\rho_s^2} d\rho_s - \frac{\beta_s}{\phi_s \rho_s} d\phi_s,$$

with T, e, ρ, η and P the temperature, specific internal energy, density, entropy and pressure, respectively, is inconsistent with the pure phase equation of state, $P_s = P_s(\rho_s, e_s)$, that BN actually use for the solid. Important consequences follow inevitably from the inclusion of ϕ_s as a thermodynamic variable, namely, (i) volume-fraction dependence also needs to appear in the solid-phase internal energy, (ii) quasistatic compaction is modeled as a reversible process, and (iii) the intergranular stress β_s emerges as a natural thermodynamic conjugate to the volume fraction. To have confidence in the model over a wide range of conditions it is important that the source terms are compatible with thermodynamics, and that each physical process is separately dissipative. Then entropy is guaranteed to be non-decreasing for every flow. Moreover, the coefficients that characterize each process (such as heat conduction or drag) can be state dependent and set or empirically fit independently.

One of the weakest aspects of currently available two-phase theories remains the manner in which they treat chemical reaction/combustion. This is an area requiring considerable study, and although we identify fruitful directions for further work, no new burn model is suggested here. The burn model of the BN theory has the notion of "hot spots" as its motivation (*i.e.*, centers of rapid reaction forced by the localization of energy at many discrete locations in the granular solid). But in effect, it is calibrated to experiments in a limited dynamical range in the phase space. It does not limit to other hot-spot motivated burn models [22] used to simulate HE initiation at higher pressures and very low porosities that fit Pop plot data for distance of run to detonation as a function of pressure. The burn model does not explicitly include the effect of the dissipation and resulting localized grain heating that occurs when the granular bed is compacted. It agrees with gas gun experiments on small HMX samples [23] only for a very limited range of impact velocities. The development of a rate model that is predictive over a wide range of conditions is a key modeling issue in need of much further investigation.

In Sec. 2 we begin with the equations that comprise the Baer-Nunziato model, and discuss the physical basis of two attributes of BN that distinguish it from conventional two-phase models, nozzling and compaction.

Also examined there are the fine-scale processes whose aggregate effect is reflected in the configuration pressure β_s, the manner in which granularity and material strength enter the constitutive theory, and the linkage of compaction-deposited energy to ignition. The dissipation inequality is the subject of Sec. 3. We emphasize its role as a constraint on constitutive modeling, and employ it to arrive at forms of the phase-interaction terms that are more general than those derived by BN. These forms allow us to correct, in Sec. 4, problems with compaction work in the BN theory. Our results are summarized in Sec. 5.

2 The Baer-Nunziato model

2.1 Postulates

The physical system envisioned in the BN model consists of a granular bed of energetic material. The intergranular pores form an interconnected region that is occupied by the gas phase. The model is postulated in accordance with the following principles of continuum-mixture theory [24]:

i) Each phase is assigned a density ρ_a, a specific volume $V_a = 1/\rho_a$, particle velocity u_a, specific internal energy e_a, temperature T_a and a volume fraction ϕ_a, where the subscript a can be either s or g, and denotes the solid and gas phase, respectively.
These variables represent the local, mesoscale material-specific average of the microscopic phase variables. The volume fractions satisfy the saturation condition, $\phi_s + \phi_g = 1$. The density and the volume fraction determine the mass fraction

$$\lambda_a \equiv \frac{\phi_a \rho_a}{\phi_s \rho_s + \phi_g \rho_g},$$

where clearly, $\lambda_s + \lambda_g = 1$.

ii) The principle of phase separation [11] holds.
We assume that on the mesoscale, each phase is in local thermodynamic equilibrium and characterized by a thermodynamic potential. Phase separation, essentially the analog of the axiom of equipresence [11] for immiscible mixtures, then dictates that the averaged, material-specific variables for each phase (*e.g.*, the Helmholtz free energy Ψ_a, the internal energy e_a, the entropy η_a, $\cdots$) depend only on the independent variables of that phase (*e.g.*, the density ρ_a, the temperature T_a, shear strain, $\cdots$). As a direct consequence of

the discrete structure of a granular solid, we include the possibility of dependence upon volume fraction, ϕ_s, in the constitutive model of the solid phase.

iii) The properties of the mixture are weighted sums of the properties of the constituents.
Quantities per unit volume, such as density (ρ) and pressure (P) are volume fraction-weighted sums of the individual phase quantities

$$\rho = \phi_s \rho_s + \phi_g \rho_g \ , \tag{1}$$
$$P = \phi_s P_s + \phi_g P_g \ , \tag{2}$$

while quantities per unit mass, such as specific internal energy (e) and specific entropy (η) are mass-weighted sums

$$e = \lambda_s e_s + \lambda_g e_g \ , \tag{3}$$
$$\eta = \lambda_s \eta_s + \lambda_g \eta_g \ . \tag{4}$$

The momentum density is volume weighted and is used to define the mixture particle velocity

$$\rho u = \phi_s(\rho_s u_s) + \phi_g(\rho_g u_g) \ , \tag{5}$$
$$u = \lambda_s u_s + \lambda_g u_g \ . \tag{6}$$

iv) Material-frame indifference holds.
The representation of the modeling PDEs and constitutive functions must be independent of the observer. For the BN model this postulate is equivalent to Galilean invariance.

v) The motion of each constituent is described by balance laws for mass, momentum and energy that are the same as those for single-phase materials. These laws can be viewed as evolution equations for the local, phase-averaged density, momentum and energy of each phase [19]. Interaction among the constituents is described by source terms, which can depend on the independent variables from both the phases.

vi) The mixture satisfies the dissipation inequality.
Each source term is constructed to model a single exchange process and these processes are separately dissipative.

vii) The modeling PDEs are evolutionary.
We require that all modifications that the exchange terms make to the basic single-phase balance laws lead to PDEs that are hyperbolic, *i.e.*, the eigenvalues for the linearized PDEs are real and the eigenvectors complete, so that the initial-boundary value problems are well-posed [25].

viii) The volume fraction ϕ_s is carried with the solid phase.
The asymmetry between the material response of the solid and gas phases motivates the advection of both ϕ_s and $\phi_g = 1 - \phi_s$, referred to as the porosity, with the solid velocity. This postulate, as we shall see, leads to the appearance of nondissipative nozzling terms in the momentum and energy equations of each phase.

2.2 Governing equations

The balance laws for the model are expressed in terms of a system of seven PDEs [12], six arising from the conservation of mass, momentum and energy for each phase, and the seventh, an evolution equation for the volume fraction, provides closure. The governing equations are:

Conservation of Mass

$$\frac{\partial}{\partial t}\left(\phi_s \rho_s\right) + \frac{\partial}{\partial x}\left(\phi_s \rho_s u_s\right) = \mathcal{C} \,, \tag{7}$$

$$\frac{\partial}{\partial t}\left(\phi_g \rho_g\right) + \frac{\partial}{\partial x}\left(\phi_g \rho_g u_g\right) = -\mathcal{C} \,; \tag{8}$$

Conservation of Momentum

$$\frac{\partial}{\partial t}\left(\phi_s \rho_s u_s\right) + \frac{\partial}{\partial x}\left(\phi_s \rho_s u_s^2 + \phi_s P_s\right) = P_N \frac{\partial \phi_s}{\partial x} + \widetilde{\mathcal{M}} = \mathcal{M} \,, \tag{9}$$

$$\frac{\partial}{\partial t}\left(\phi_g \rho_g u_g\right) + \frac{\partial}{\partial x}\left(\phi_g \rho_g u_g^2 + \phi_g P_g\right) = -P_N \frac{\partial \phi_s}{\partial x} - \widetilde{\mathcal{M}} = -\mathcal{M} \,; \tag{10}$$

Conservation of Energy

$$\frac{\partial}{\partial t}\left(\phi_s \rho_s E_s\right) + \frac{\partial}{\partial x}\left[\phi_s u_s (\rho_s E_s + P_s)\right] = P_N u_s \frac{\partial \phi_s}{\partial x} - P_c \mathcal{F} + \widetilde{\mathcal{E}} = \mathcal{E} \,, \tag{11}$$

$$\frac{\partial}{\partial t}\left(\phi_g \rho_g E_g\right) + \frac{\partial}{\partial x}\left[\phi_g u_g (\rho_g E_g + P_g)\right] = -P_N u_s \frac{\partial \phi_s}{\partial x} + P_c \mathcal{F} - \widetilde{\mathcal{E}} = -\mathcal{E} \,; \tag{12}$$

Compaction dynamics

$$\frac{\partial \rho_s}{\partial t} + \frac{\partial (\rho_s u_s)}{\partial x} = -\frac{\rho_s}{\phi_s}\mathcal{F} \ . \tag{13}$$

Here, the left hand sides of Eqs. (7)–(13) are shown in conservation form and $E_a = e_a + u_a^2/2$ is the total specific energy. The right-hand sides of Eqs. (7)–(12) are source terms that characterize phase interaction. These terms correspond to mass ($\mathcal{C}$), momentum ($\mathcal{M}$) and energy ($\mathcal{E}$) transfer between the phases. The mass source $\mathcal{C}$ is negative when the solid burns and is converted to gas. The total mass, total momentum and total energy are all conserved because the source terms for the gas and solid phases sum to zero. As we show later, the right-hand side of Eq. (13) describes the rate of compaction. The eigenvalues of this system of equations are all real. Except for isolated surfaces in the state space, the linearly non-degenerate characteristic velocities are unequal and the eigenvectors are complete so that effectively, the PDEs are hyperbolic [21].

Some general remarks about the governing equations, and the quantities appearing therein, are in order. In the continuum approximation the phases coexist at each point. The individual phase variables can be viewed as local, mesoscale averages over a subvolume that is large enough to contain a sufficient number of grains so that the local volume average is statistically meaningful. Underlying this view are two implicit assumptions. First, that self-equilibration of each phase occurs at a rate much faster than that at which the phases seek equilibrium with each other. Second, that the agents forcing changes in the system, such as pressure gradients, themselves vary on the mesoscale rather than the grain scale. The formal averaging approach, long advanced by Drew [19], provides some justification for this view, as we now argue.

Let $\langle \ \ \rangle_\ell = \int (\ ) dV/V_\ell$ be the ℓ-scale volume averaging symbol, where ℓ denotes the continuum or mesoscale. Given an indicator function $X_a \equiv \{0, 1\}$, where $X_a = 1$ in regions of space occupied by material a and zero otherwise, then $\langle X_a \rangle_\ell = \phi_a$. Upon averaging, the standard, microscale conservation equations yield their "averaged" or weighted counterparts that parallel the standard pure-phase equations [19]. Unlike the latter, however, the averaged equations contain source terms that reflect the fact that for a nonlinear function, $\langle f(x, y, \cdots) \rangle_\ell \neq f(\langle x \rangle_\ell, \langle y \rangle_\ell, \cdots)$. These sources represent interactions both between the phases and within each phase, appearing as (a) forces and fluxes that act across the interfacial boundaries and (b) averages of products of fluctuations from the mean fields within each phase.

An example of the former are the forces established within grains due to intergrain contacts and of the latter, intraphase pressure fluctuations.

Here we focus on an issue not addressed by Drew; how the nonlinear constitutive model for e_a comes through the averaging when the forces driving changes on the ℓ-scale are simple compressions. We consider that on the microscale the response of the solid, $\tilde{e_s}(\overline{\overline{\epsilon}}, T; \alpha_k)$ is complex; acting thermoelastically at low pressures and plastically at high pressures. In the above, $\overline{\overline{\epsilon}}$ is the strain tensor and the α_k are added (hidden) internal state variables that are needed to describe the transition from elastic to inelastic response [26]. Three time scales enter the problem: a short, fundamental acoustic time t_c based on the grain dimension, a longer evolution time $t_\ell >> t_c$ based on the ℓ-scale and a process time scale $t_\alpha >> t_c$ that characterizes the rates of change of the hidden variables α_k. Here we focus on the limit $t_\alpha > t_\ell$.

At first glance, the nonlinear dependence of the microscale, pure-phase solid EOS function $\tilde{e_s}$ on $\overline{\overline{\epsilon}}$, T and α_k would result in $\langle X_s \rho \tilde{e_s}(\overline{\overline{\epsilon}}, T; \alpha_k)\rangle_\ell \neq \langle X_s\rho\rangle_\ell \tilde{e_s}(\langle\overline{\overline{\epsilon}}\rangle_\ell, \langle T\rangle_\ell; \langle\alpha_k\rangle_\ell)$. Given $t_c << t_\ell$ and the smoothness of the applied forces on the ℓ-scale, the fluctuations in the strain and temperature fields within each grain are short-lived, while the α_k are frozen since $t_\alpha > t_\ell$. Therefore, the fields evolve quasisteadily on the ℓ-scale. When the grains are <u>isolated</u>, this leads to <u>uniform</u> fields and a bulk response within grains, since the load they experience is hydrostatic. Then, $\langle X_s\rho\ \tilde{e_s}(\overline{\overline{\epsilon}}, T; \alpha_k)\rangle_\ell = \langle X_s\rho\rangle_\ell\ \tilde{e_s}(\langle\rho\rangle_\ell, \langle T\rangle_\ell; \langle\alpha_k\rangle_\ell)$, where $\langle\overline{\overline{\epsilon}}\rangle_\ell = \langle\rho\rangle_\ell$, since the average shear strain $\langle S(\overline{\overline{\epsilon}})\rangle_\ell$ is zero for a hydrostatic load. When the grains are in <u>contact</u>, the fields in the grains, although quasisteady, are <u>nonuniform</u> due to the localized nature of the grain-to-grain contacts. Then the average shear strain $\langle S(\overline{\overline{\epsilon}})\rangle_\ell \neq 0$, so that $\langle X_s\rho\ \tilde{e_s}(\overline{\overline{\epsilon}}, T; \alpha_k)\rangle_\ell \neq \langle X_s\rho\rangle_\ell\ \tilde{e_s}(\langle\rho\rangle_\ell, \langle T\rangle_\ell; \langle\alpha_k\rangle_\ell)$. Since $\langle S(\overline{\overline{\epsilon}})\rangle_\ell$ is not a variable in this continuum theory, to close the model we approximate $\langle X_s\rho\ \tilde{e_s}(\overline{\overline{\epsilon}}, T; \alpha_k)\rangle_\ell$ simply as $\tilde{e}_{sp}(\langle\rho\rangle_\ell, \langle T\rangle_\ell; \langle\alpha_k\rangle_\ell) + g(\phi_s, \cdots; \langle\alpha_k\rangle_\ell)$, where $\tilde{e}_{sp}$ is the mesoscale hydrostatic contribution, and $g(\phi_s, \cdots; \langle\alpha_k\rangle_\ell)$ represents, in an average way, the effects on the mesoscale internal energy of the microscale shear strain $\langle S(\overline{\overline{\epsilon}})\rangle_\ell$ (which is related to the degree of compaction, ϕ_s). Similar arguments for the gas phase yield $\langle X_g\rho e_g(\rho, T)\rangle_\ell = \langle X_g\rho\rangle_\ell e_g(\langle\rho\rangle_\ell, \langle T\rangle_\ell)$. Thus, the microscale material response to simple compressions is used as the mesoscale EOS, with an added term to reflect the effects of the averaged localized strains.

Next we turn to a related quantity that appears in the theory as a result of grain-to-grain interaction. Intergrain contacts produce strains that lead to contact stresses, displayed in Figure 1 as gray shaded regions with the lightest gray indicating the highest stress. These stresses are manifest in

the BN-theory as a continuum-level configuration pressure, or intergranular stress,

$$\beta_s(\phi_s, \cdots; \langle\alpha_k\rangle_\ell) \ .$$

Dependence on ϕ_s is natural, as already remarked. The solid phase experiences both the pressure carried by the gas, denoted by arrows in Figure 1, and the intergranular forces. At mechanical equilibrium, $P_s = P_g + \beta_s$.

The configuration pressure and $g(\phi_s, \cdots; \langle\alpha_k\rangle_\ell)$ play a significant role at low pressure when the solid phase is stiff relative to the gas. The pressure above which material strength becomes unimportant is referred to as the crush-up pressure and is of the order of the yield strength; at the crush-up pressure the pores in a granular bed are nearly squeezed out as the solid becomes fluid-like. A porous bed of granular HMX achieves 1% porosity for $\beta_s \approx 5$ kbar; we say that the crush-up pressure for HMX is about 5 kbar.

We begin a discussion of the compaction equation by observing that in the BN model, the volume fraction ϕ_s serves multiple purposes. Besides being a measure of the strain induced in the grains, it is also the variable that describes the microstructure of the interface separating the phases. The theory of Passman, Nunziato and Walsh [11], on which the BN model is based, postulates an evolution equation for the microstructure. Such concepts as "microstructural inertia" and "microstructural force" are introduced to model the evolution of ϕ_s with a second-order PDE of the form

$$(\text{microinertia}) \cdot \frac{d^2\phi_s}{dt_s^2} + (\text{viscosity}) \cdot \frac{d\phi_s}{dt_s} = (\text{microstructural forces}) \ , \quad (14)$$

where d/dt_s is the convective derivative with respect to the solid. In spirit this equation is similar to the pore-collapse model of Carroll & Holt [27], although its development was couched in a "Rational Mechanics"-type formalism [11], [28]. In their model, Baer and Nunziato [12], in effect, set the microinertia to zero and obtain closure by simply postulating the existence of a constitutive expression relating $d\phi_s/dt_s$ to the independent variables of both phases,

$$\frac{d\phi_s}{dt_s} = \mathcal{F}(\rho_s, \rho_g, P_s, P_g, \phi_s, \cdots) \, , \quad (15)$$

where $\mathcal{F}$ is meant to mimic the effects of microstructural forces that, on the continuum level, describe the "resistance" exhibited by the bed to changes in its configuration. The form that BN derive is

$$\mathcal{F} \ = \ \frac{\phi_s \phi_g}{\mu_c} \Big(P_s - \beta_s - P_g \Big) \, , \quad (16)$$

where the parameter μ_c is called the compaction viscosity due to the analogy with Eq. (14).

Turning now to the source terms, we have separated out, from the momentum and energy transfer rates, contributions that were developed by BN. These include the nozzling terms, proportional to P_N, and the compaction-work terms, proportional to P_c. BN take the nozzling pressure to be the gas pressure, *i.e.*,

$$P_N = P_g, \tag{17}$$

and the compaction pressure to be the difference of the solid pressure and the configuration pressure, *i.e.*,

$$P_c = P_s - \beta_s. \tag{18}$$

We shall examine both of these terms in some detail shortly. The residual momentum exchange $\widetilde{\mathcal{M}}$ and the residual energy exchange $\widetilde{\mathcal{E}}$ used by BN are

$$\widetilde{\mathcal{M}} = \mathcal{C}\, u_s + (\delta + \frac{1}{2}\mathcal{C})(u_g - u_s)\,, \tag{19}$$

$$\widetilde{\mathcal{E}} = \mathcal{C}\,(e_s + \frac{1}{2}\,u_s^2) + (\delta + \frac{1}{2}\,\mathcal{C})\,u_s\,(u_g - u_s) + \mathcal{H}\,(T_g - T_s)\,. \tag{20}$$

Equation (19) is the BN form for the momentum exchange associated with burning and drag, while equation (20) describes the energy exchange due to burning, drag and heat transfer. The coefficients δ and $\mathcal{H}$ appearing in (19) and (20) are, respectively, the interphase drag and heat transfer coefficients.

In the remainder of this section we examine the constitutive modeling of the phase-specific quantities. We start by briefly discussing the compaction law and the nozzling term.

2.3 Compaction and nozzling

In contrast to typical two-phase fluid models [29], the BN-model does not require the phases to be in pressure equilibrium. Instead, pressures are related dynamically via the compaction law, Eq. (13). Conservation of solid mass, Eq. (7), allows the compaction equation to be cast in a more standard form as

$$\frac{d\phi_s}{dt_s} - \frac{\mathcal{C}}{\rho_s} = -\left[\frac{\partial \rho_s}{\partial t} + \frac{\partial(\rho_s\, u_s)}{\partial x}\right]\frac{\phi_s}{\rho_s} = \mathcal{F}\,. \tag{21}$$

Here, ϕ_s advects with the solid phase, and the source $\mathcal{F}$ measures the rate of compaction. Without burn, the equilibrium value of ϕ_s is given by $\mathcal{F} = 0$

and corresponds to $P_s = P_g + \beta_s$. Thus, the compaction equation serves as a relaxation law that drives the phases towards pressure equilibrium, with the compaction viscosity μ_c characterizing the relaxation rate. A favorable consequence of pressure non-equilibrium is that the model equations are hyperbolic, rather than of the mixed hyperbolic-elliptic variety typical of two-phase pressure-equilibrium models [29].

At low pressures the grains are nearly incompressible, *i.e.*, $\rho_s \approx$ constant. Then, for a nonreactive system, the compaction law reduces to

$$\frac{d\phi_s}{dt_s} = -\phi_s \frac{\partial u_s}{\partial x}\,, \tag{22}$$

and the solid pressure is determined by $-\phi_s \partial u_s/\partial x = \mathcal{F}$. Eq. (22) also corresponds to the incompressible limit of the equation for mass conservation of the solid; in this limit, therefore, compaction is simply a statement of mass conservation, *i.e.*, compaction is due to the relative solid-to-solid motion which reduces the volume of the pores within the bed.

The asymmetric form of compaction dynamics in the BN model (biased towards the solid), along with the dissipation inequality, forces the appearance of the nozzling term, $P_N \partial\phi_s/\partial x$, in the momentum and energy equations (see Sec. (3)). The change in porosity on the continuum scale acts as a nozzle which can either accelerate or decelerate the gas flow and drive relative motion between the phases. At pressures below the crush-up pressure of the granular bed, such a porosity gradient can be set up, for example, across a compaction wave. Figure 2 shows the manner in which a gradient in porosity (produced by the gradient in the number density of grains, with a higher grain density indicated as darker) acts on the continuum scale like a nozzle. Nozzling accounts for the average effect of the solid interface on the gas flow. When the pressures are equal, $P_N = P_g = P_s$, the nozzling term corresponds to the PdV work one phase does on the other when the internal phase interface varies and changes the volume fraction.

Nozzling terms are included in some two-phase mixture models [19] and discarded in others [16]. They prevent the BN equations from being put in a conservative form. This does not cause any problems provided the initial porosity is continuous, since the PDEs have a well-defined wave structure that maintains continuity of ϕ_s [21]. In Sec. (3.2) we show that the nozzling term is required in order to guarantee that entropy is non-decreasing for all flows.

Nozzling plays a role at low pressure when the solid phase is stiff relative to the gas, and for it to have a significant effect on the gas flow, drag must be

small. At high pressure the solid becomes more fluid-like, drag becomes large and nozzling diminishes in importance. Even at low pressures, when the ambient mass fraction of the gas is small, the solid EOS and the configuration pressure β_s are sufficient to predict low pressure compaction waves in a granular bed, that is, the lead compaction wave in a DDT experiment is insensitive to the nozzling terms. An example of the effect of nozzling on a piston driven compaction wave is shown in [3].

2.4 Equilibrium thermodynamic response

As discussed above, the BN theory [12] treats the explosive as a mixture of phase-separated substances [11]. Constitutive relations must be provided for the phase-specific quantities such as the Helmholtz free energy Ψ_a, and for the phase-interaction or exchange terms such as $\mathcal{C}$, $\mathcal{M}$ and $\mathcal{E}$. In this section, we concentrate on expressions for the averaged phase-specific, thermodynamic response. These expressions describe how each phase interacts with itself, including the ways in which granules interact across their interfaces. Intraphase response such as friction and viscosity could be included in the interphase response, although the BN theory omits such processes.

The material-specific phase response functions are constructed according to the postulates enunciated at the beginning of this section, including in particular, the principles of material frame indifference and phase separation. Thus, Ψ_a is taken to depend on the independent variables $\rho_a,\ T_a,\ \phi_a, \cdots$, where the dependence on the volume fraction accounts for the energy associated with the intergrain contacts.

Continuum mixture theory has been applied to many types of materials [30, 31], including solids for which the stress and strain tensors are important variables. The BN model is aimed at describing a granular bed. In contrast to a pure solid, large shear strains do not necessarily give rise to large shear stresses because grains can slide past each other. This motivates replacing the stress tensor by a hydrostatic pressure and the strain tensor by a density. Material strength is modeled with the configuration pressure introduced earlier and discussed below. Thus, the BN model is a fluid-like model, and the set of independent variables is restricted to $S_a \equiv (\rho_a, T_a, \phi_a)$. Since all the variables are scalars, material frame indifference reduces to Galilean invariance.

With the variable list S_a, the derived thermodynamic variables are the

entropy

$$\eta_a = -\left(\frac{\partial \Psi_a}{\partial T_a}\right) , \tag{23}$$

the internal energy

$$e_a = \Psi_a + T_a\, \eta_a , \tag{24}$$

the pressure

$$P_a = \rho_a^2 \left(\frac{\partial \Psi_a}{\partial \rho_a}\right) , \tag{25}$$

and the intergranular stress or configuration pressure

$$\beta_a = \phi_a\, \rho_a \left(\frac{\partial \Psi_a}{\partial \phi_a}\right) . \tag{26}$$

Since a gas has no material strength, β_g is zero, *i.e.*, the free energy of the gas has the pure single phase form $\Psi_g(\rho_g, T_g)$.

We start by exploring the consequences of the ϕ_s-dependence. The volume fraction is an internal degree of freedom which can be externally set only indirectly through an applied pressure. It is natural to enquire about the equilibrium volume fraction for a porous solid according to the above constitutive model, as determined by maximizing the entropy for a fixed solid mass, energy and volume, *i.e.*, for e_s and $\rho = \phi_s \rho_s$ constant. The solid thermodynamic variables satisfy the differential relation

$$de_s = \frac{P_s}{\rho_s^2} d\rho_s + T_s d\eta_s + \frac{\beta_s}{\phi_s \rho_s} d\phi_s . \tag{27}$$

Since the constraints imply that $de_s = 0$ and $d\rho_s/\rho_s = -d\phi_s/\phi_s$, it follows that at equilibrium, $P_s = \beta_s$. Thus, a direct consequence of the ϕ_s-dependence of Ψ_s is the emergence of β_s to describe the resistance of a granular bed to compaction under an applied pressure P_s. Since the grains are not bonded together, the granular bed cannot support tension and the configuration pressure must be positive.

We now turn to the question of consistently constituting the functional form for the equilibrium response. Due to the effects associated with material strength, the response of a granular bed is complex. As already observed, the small contact surfaces over which the grains interact can lead to large stress concentrations even under moderate loads. Grains can fracture, and when the local stresses exceed the yield strength, deform plastically. The resulting changes in microstructure affect the distribution of grain sizes and contacts among grains. As a result, small grains can then be squeezed

through pores between larger grains, giving rise to frictional heating. Thus, in addition to hydrostatic pressure arising from density changes, contact stresses may lead to (i) elastic deformations, (ii) fracture, (iii) intergranular friction, and (iv) plastic deformation. Since some of these processes are irreversible, they lead to hysteresis effects or different paths in state space when a granular bed is loaded and unloaded.

The relative mix of reversible and irreversible processes is material-dependent. For example, compaction of ball propellants is dominated by (i) rearrangement, (ii) elastic loading and finally (iii) plastic deformation [32]. Little or no fracture is observed. On the other hand, compaction of granular HMX is dominated by fracture [33]. This complexity of material response poses a significant challenge to the micromechanical modeler.

In principle, given a sufficiently capable micromechanical code, physically accurate material models and a knowledge of the local microstructure, the fields derived from a micromechanical simulation could be averaged to obtain the continuum scale response function. Though valid in principle, this approach is impractical, at least in a quantitative sense, given the present state of the art. A semi-empirical construction, guided by qualitative information gathered from averaging, and buttressed by a judiciously selected suite of calibration experiments, is more likely to succeed. In either case, additional variables besides ϕ_s are sure to be needed to characterize the material state in all its complexity, along with evolutionary equations for these variables. Models more like those used to describe plastic or viscoelastic behavior, that express stress rate in terms of strain rate, could lead to improved descriptions. Such extended constitutive models are currently under development for granular explosive materials; see Gonthier *et al.* [34], [35].

Here we follow BN and continue with the prescription where ϕ_s is the only additional state variable in what is otherwise a fluid equation of state, keeping in mind that while such a continuum model cannot capture all the details, upon proper calibration it can describe states of mechanical equilibrium and the gross energetics for a class of applications. We seek to calibrate $\Psi_s(\rho_s, T_s, \phi_s)$ to data on compressive loading of granular beds [36]. In these experiments, a uniform load is applied slowly to a thermally isolated, well-characterized bed of granular HMX with little gas (ambient air). This results in a uniform, quasistatic compaction of the bed, and serves to measure how the internal energy of the bed increases on compaction, as we now show.

The control variable in the experiments described above is the volume occupied by the porous HMX. A platen, of area A and initially a distance

L_0 from the far side of the sample cell, is moved slowly into the bed so as to uniformly compress the bed. Since the pressure required to compress the bed is sufficiently low, the volume ν_s of the solid grains remains roughly constant and $\rho_s = (m_s/\nu_s) = \rho_s^0$, where the solid volume fraction is $\phi_s = (\nu_s/A \cdot L)$. The bed remains uniform due to the slowness of compaction, so that

$$\frac{d\phi_s}{dt} = -\frac{A\phi_s^2 \cdot (u_s)_L}{\nu_s} \,, \tag{28}$$

where $(u_s)_L = dL/dt$ is the platen velocity. Since the solid is the only component, the solid energy equation Eq. (11), free of source terms, can be integrated to get the change in energy of the material,

$$\int_0^L \frac{\partial(\phi_s \rho_s E_s)}{\partial t} A dx + (\phi_s u_s (\rho_s E_s + P_s))_L \, A = 0 \,. \tag{29}$$

Bringing the time derivative through the integral

$$\int_0^L \frac{\partial(\phi_s \rho_s E_s)}{\partial t} A dx = \frac{d}{dt} \int_0^L (\phi_s \rho_s E_s) A dx - u_s \cdot (\phi_s \rho_s E_s)_L A$$

and using $d/dt = (d\phi_s/dt) d/d\phi_s$ leads to

$$\frac{d}{d\phi_s} \int_0^L (\phi_s \rho_s E_s) dx = \frac{\nu_s \cdot (P_s)_L}{A\phi_s} \,. \tag{30}$$

This can be integrated to obtain

$$e_s - e_s(\rho_s^0, \phi_s^0) = B = \int_{\phi_s^0}^{\phi_s} \frac{(P_s)_L}{\rho_s \phi_s} d\phi_s \,, \tag{31}$$

where the kinetic energy of compaction has been neglected. Since ρ_s is essentially unchanged in the loading experiment, and $(P_s)_L$ is observed to principally depend on ϕ_s, it is reasonable to treat B as a function of ϕ_s alone. We can identify $(P_s)_L$ with β_s, *i.e.*,

$$(P_s)_L = \beta_s = \phi_s \rho_s \frac{dB(\phi_s)}{d\phi_s} \,. \tag{32}$$

The quantity β_s is the intergranular stress as measured in the quasistatic compaction experiments of Elban & Chiarito [36]. (These experiments measure the applied force on the platen, $F = A\phi_s\beta_s$ which needs to be reduced by 40% to account for the load carried by friction at the mold wall.) We

exclude the possibility of a dependence of β_s on T_s; more due to a lack of information. Although, as T_s is increased sufficiently, we expect that thermal softening can strongly influence the measured $(P_s)_L$.

We identify the change in energy $B(\phi_s)$, given in Eq. (31), with the compaction energy

$$B(\phi_s) = \int_{\phi_s^0}^{\phi_s} \frac{\beta_s}{\rho_s \phi_s} d\phi_s \ . \tag{33}$$

With the T_s-dependence of β_s neglected and $\rho_s \approx$ constant, B is the change in the internal energy of the bed on loading, and describes phenomenologically the low-pressure, quasistatic, compressive loading of the bed.

Given this change in the energy of the bed, we are at liberty as to how to represent this as a change in the internal energy of the solid. Here, following the BN formalism, we elect to associate all of this energy with a reversible process, such as elastic deformation in the vicinity of grain contacts. That would imply that neither the temperature nor the density of the solid grains had changed during compaction, and the internal energy would have the form $e_s(\rho_s, T_s, \phi_s)$, with ϕ_s as an added internal-state variable to measure the change in energy. With this ansatz, the intergranular stress, β_s has a thermodynamic definition as the force conjugate to the internal-state variable ϕ_s. From Eq. (27) it follows that for the assumed constant density process, the change in solid entropy for a quasistatic process would be zero with the reversible ansatz.

With ϕ_s adopted as an internal-state variable, we seek to develop a consistent theory that treats B as an approximation to the free energy of the bed for low pressure loading. In BN, the intergranular stress derived from B is the only way in which material strength and granularity enter into the constitutive theory of the solid. The fits to the experimental data of Elban & Chiarito for HMX are shown in Figure 3. We note that β_s is relatively insensitive to the grain distribution and packing of the bed, except near ambient pressure. The experiments also indicate that a single function approximately describes the progressive crush-up of the bed, even for a loading cycle that involves unloading followed by reloading during the cycle.

As the pressure increases beyond the yield strength of solid HMX, then $\beta_s/P_s << 1$ and B represents only a small part of the total energy. Then the material response is dominated by the fluid-like, continuous pure phase solid EOS, $\Psi_{sp}(\rho_s, T_s)$. The composite EOS

$$\Psi_s(\rho_s, T_s, \phi_s) = \Psi_{sp}(\rho_s, T_s) + B(\phi_s) \ , \tag{34}$$

captures both the low and high pressure response of granular HMX to compressive loading and so reperesents an accurate and robust approximation over a wide range of conditions. It is consistent with the thermodynamic description given earlier in this subsection with

$$
\begin{aligned}
e_s &= e_{sp} + B \ , && (35)\\
\eta_s &= \eta_{sp}(\rho_s, e_{sp}) \ , && (36)\\
P_s &= P_{sp}(\rho_s, e_{sp}) \ , && (37)\\
e_{sp} &= \Psi_{sp} + T_s \eta_s \ . && (38)
\end{aligned}
$$

In particular, in this description there is no additional entropy associated with generation of grain surfaces, friction and plastic deformation that can accompany quasistatic compaction.

The total energy supplied to compact the bed can be computed using the data of Figure 3 and the expression for $B(\phi_s)$. For a typical quasistatic experiment it is of order 1×10^4 J/kg. Here we give some estimates of the energy that could be associated with two processes described above and which can be expected to occur during compaction (one reversible and the other irreversible): (i) elastic deformation and (ii) fracture. Based on the low values of these energies relative to the compaction energy, we argue that for HMX a significant fraction of the compaction energy can be accounted for by the intergranular friction that accompanies the rearrangement of the fractured grains. Given the highly irreversible nature of this process, we examine data on HMX gathered by Coyne, Elban & Chiarito [36] that shows the extent of the irreversibility.

The elastic shear-strain energy for an isotropic linearly elastic material is $Y^2/(6G\rho_0)$, where Y is the yield strength and G is the shear modulus. For HMX the maximum shear-strain energy is 8×10^2 J/kg, based on $Y = 0.3$ GPa and $G = 10$ GPa. This is an order of magnitude smaller than the compaction energy. Given that this is an overestimate, since only a small fraction of each grain experiences these forces, it is unlikely that shear-stress is an energetically important mechanism.

The energy associated directly with fracture is of the order of 2 J/kg. This is based on the estimate of $0.05\,\mathrm{J/m^2}$ for surface energy of HMX [37] and the surface area per unit mass for grains 0.1 mm in diameter. Although fracture has no direct influence on the HMX compaction energetics, the effects of intergranular friction that accompany the rearrangement of fractured grains can impact the energetics significantly. As mentioned above, the experiments of Elban & Chiarito [36] reveal that upwards of 40% of the

load applied to compact a bed on the platen is carried by friction between the HMX grains and the smooth walls of the cylinder used to confine the bed. All of the above argue that compaction is highly irreversible and that plastic deformation and intergranular friction play important roles in the quasistatic compaction of granular HMX.

The experiments of Coyne, Elban & Chiarito [36] show a hysteresis effect for the loading and unloading response of HMX. A representative $\phi_s\beta_s$ vs $1/\phi_s$-diagram is shown in Figure 4, for a sample initially at $\phi_s^0 = 0.73$. In these variables, the area under the curve corresponds to the compaction energy, Eq. (33). Also shown in Figure 4 are two unloading curves (corresponding to release isentropes) from states of compaction $\phi_s = 0.95$ and $\phi_s = 0.85$ and labeled $\mathcal{A}$ and $\mathcal{B}$, respectively. A measure of the degree of reversibility of the compaction process is the ratio of the area below the unloading curve to the area below the loading curve. The small ratio implies that the energy dissipated as heat by irreversible processes is a large fraction of the total compaction energy for HMX. These results are compatible with the low values we obtained for the energy estimates (given above).

Alternatively, if we deem that compaction is fully irreversible, and that the entire energy associated with compaction is dissipated, then we would need to associate this energy with a change in T_s, and constitute the internal energy as simply $e_s(\rho_s, T_s)$. We discussed this possibility in Sec. (2.2) with the introduction of the hidden EOS variables α_k. From Eq. (27) it follows that the change in solid entropy would be positive if compaction were assumed to be irreversible. This would correspond to the limit $t_\alpha < t_\ell$. We could of course assign a fraction of B to reversible processes and the remainder to irreversible ones. Improvements in the modeling are needed to capture this added dissipation along the lines of elastic-plastic theory [34], [35].

Because of its historical interest, we relate our results to those of the "$P - \alpha$" model of Herrmann [38] and Carroll & Holt [39]. When no gas is present, the pressure of the mixture in the $P - \alpha$ model is given by

$$P = \phi_s P_{sp}(\rho/\phi_s, e_{sp}) \, ,$$

which is equivalent to Eq. (37). However, $e_s = e_{sp}$ in the $P-\alpha$ model, so the energy of quasistatic compaction is fully dissipated. Since ϕ_s is assumed to equilibrate instantly in response to the applied pressure (*i.e.*, $\phi_s(P, \rho_s = \rho_s^0)$), compaction waves are not dispersive and no added dissipation (over and above that expected for a shock) enters the model due to dynamic processes such as compaction waves.

For our modified BN model, the theoretical description of $B(\phi_s)$ does not account for any of the dissipative heating, to be sure. However, it is only the dissipation associated with quasisteady compaction that is absent. Since compaction is modeled as a dynamic process in this description, Eq. (21), dissipation due to the non-equilibrium nature of the compaction process is indeed allowed and can be significant, as we show in the following section.

2.5 Compaction energy and ignition

We now examine the energetics of compaction and the manner in which compaction is linked to the initiation of combustion in a loosely-packed bed. During the passage of a compaction wave, a substantial decrease in the volume of the bed results in work being done on the bed. With only solid present, this leads to an increase in the internal energy of the solid grains that is significantly greater than that produced by a shock of comparable strength in a full-density solid. Unlike quasistatic compaction examined in the previous section, the compaction wave is a dynamic, irreversible process and so always generates entropy. For the low-velocity impacts on granular HMX explosive that are considered likely accident scenarios, the pressures induced in the bed are seldom above the crush-up pressure of the bed. Thus, although the increase in internal energy in the granular solid exceeds that obtained in full-density solid, the increase is still not particularly large, and the corresponding rise in the bulk temperature alone is insufficient to initiate combustion. The increase in internal energy also comes from a variety of sources, and this puts an added burden on the modeler to faithfully describe the various dissipation mechanisms that can be present during the compaction of a granular bed. For the high-velocity impacts more typical of prompt shock initiation, the pressures and consequently the work done in compacting and heating the bed are one to two orders of magnitude greater, leading to the bulk solid temperature being many hundreds of degrees higher. This leads to the onset of rapid and wide-spread combustion in the bulk of the solid grains. Such high-velocity impacts are not of interest for the explosive safety problem which motivates this study. One concludes, therefore, that for granularity to play a role in low-speed impacts, some form of energy localization or "hot-spot" formation is required to reflect the combustion observed experimentally in such situations.

To illustrate some of the issues involved, we consider the propagation of a one-dimensional compaction wave in gas-free ($\rho_g = 0$) granular bed. To have all the momentum and energy generated by the compaction wave

directed at the solid, we set $P_N = P_c = P_g = 0$, $\delta = 0$ and $\mathcal{C} = 0$ in the model. In this gasless limit, the applied or mixture pressure and mixture density are, respectively,

$$P = \phi_s \, P_s \qquad \text{and} \qquad \rho = \phi_s \, \rho_s \; .$$

The jump conditions across such a wave traveling at a constant speed D are obtained from the conservation of mass, momentum and energy, as

$$\begin{aligned} \rho(u_s - D) &= -\rho^0 \, D \; , \\ P - P^0 &= \rho^0 \, D \, u_s \; , \\ e_{sp} - e^0_{sp} + B - B^0 &= \frac{1}{2} \left(\frac{1}{\rho^0} - \frac{1}{\rho} \right) (P + P^0) \; . \end{aligned} \tag{39}$$

In addition, the state behind the compaction wave is assumed to be in mechanical equilibrium, *i.e.*,

$$P_s = \beta_s \; .$$

Two constitutive expressions are needed to completely define the compaction wave: a prescription for the configuration pressure β_s, and an equation of state for the solid phase. Both are based on HMX-data gathered from experiments.

In order to quantify the compaction energetics one turns to the Hugoniot condition for energy, the third equation of set (39). First, as is appropriate for weak waves, it is convenient to replace $e_{sp} - e^0_{sp}$ by its linearization about the initial state,

$$e_{sp} - e^0_{sp} = \mathcal{A} \cdot \left(\frac{P_s - P^0_s}{P^c_s} \right) + \mathcal{B} \cdot \left(\frac{\rho^0_s}{\rho_s} - 1 \right) + \cdots \; . \tag{40}$$

Here, pressure is scaled in units of the crush-up pressure P^c_s, and

$$\mathcal{A} \equiv \frac{P^c_s}{\rho^0_s \, \Gamma^0_s} \; , \qquad \mathcal{B} \equiv \frac{(c^0_s)^2}{\Gamma^0_s} - \frac{P^0_s}{\rho^0_s} \; ,$$

where Γ^0_s and c^0_s are the Gruneisen parameter and sound speed at ambient conditions, respectively. Second, we employ the decomposition

$$\frac{1}{\rho^0} \left(1 - \frac{\rho^0}{\rho} \right) = \left(\frac{1}{\rho^0_s} - \frac{1}{\rho_s} \right) \frac{1}{\phi_s} + \frac{1}{\phi^0_s \, \rho^0_s} \left(\phi_s - \phi^0_s \right) \frac{1}{\phi_s} \; .$$

Then, with the initial pressure neglected, the energy Hugoniot in Eq. (39) takes the form

$$\begin{aligned} \mathcal{A}\cdot\left(\frac{P_s}{P_s^c}\right) \quad &+ \quad \mathcal{B}\cdot\left(\frac{\rho_s^0}{\rho_s}-1\right)+B-B^0\cdots \\ &= \quad \frac{P_s}{2\,\rho_s^0}\left(1-\frac{\rho_s^0}{\rho_s}\right)+\frac{P_s}{2\,\rho_s^0}\left(\frac{\phi_s}{\phi_s^0}-1\right)\ . \end{aligned} \tag{41}$$

The work done on the solid by both compressing the solid grains and compacting the bed are clearly separated on the right hand side, being represented by the first and second terms, respectively.

Our estimates on the response of HMX use the Helmholtz free energy EOS for pure solid HMX that has been calibrated by Gustavsen & Sheffield [23]. For this EOS, the coefficient $\mathcal{B}$ is given by

$$\mathcal{B}\equiv C_{vs}T_s^0\Gamma_s^0+\frac{K_s^0}{\rho_s^0\Gamma_s^0}\ ,$$

where the constants for HMX at the ambient temperature of $T_s^0 = 300\,\mathrm{K}$ and $P_s^0 = 0$ are the specific heat, $C_{vs} = 1.05\times10^{-6}\,\mathrm{GPa\cdot m^3/(kg\cdot K)}$, the isothermal bulk modulus, $K_s^0 = 12.9\,\mathrm{GPa}$, $\rho_s^0\Gamma_s^0 = 2090\,\mathrm{kg/m^3}$ and $\rho_s^0 = 1900\,\mathrm{kg/m^3}$. With $P_s^c = 0.5\mathrm{GPa}$, we obtain $\mathcal{A} = 2.4\times10^{-4}\,\mathrm{GPa\ m^3/kg}$ and $\mathcal{B} = 6.5\times10^{-3}\,\mathrm{GPa\ m^3/kg}$. Furthermore, for $P_s\le P_s^c$, B is at most 8.27×10^{-6} GPa m^3/kg and $P_s/(2\rho_s^0)$ no larger than 1.32×10^{-4} GPa m^3/kg. Thus, $\mathcal{A}$, B and $P_s/(2\rho_s^0)$ are at least an order of magnitude smaller than $\mathcal{B}$. Since P_s/P_s^c and $(\phi_s-\phi_s^0)$ are both of order unity for the weak compaction waves under consideration, Eq. (41) implies that to leading order,

$$1-\frac{\rho_s^0}{\rho_s}=O\left(\frac{\mathcal{A}}{\mathcal{B}}\right)\ll 1\ .$$

Consequently, below the crush-up pressure, the jump conditions for a compaction wave do not depend on the details of the energy equation (since $\rho_s\approx\rho_s^0$) and are given simply by

$$\begin{aligned} \phi_s(u_s-D) &= -\phi_s^0\,D\ , \\ \phi_s\,P_s &= \phi_s^0\,\rho_s^0\,Du_s\ , \\ P_s &= \beta_s(\phi_s,\rho_s=\rho_s^0)\ . \end{aligned} \tag{42}$$

The important point here is that the lead compaction wave is insensitive to the energetics of the flow [40]; any uncertainty with regard to the appropriate

form for the EOS for a granular solid (*e.g.*, should an explicit ϕ_s-dependence be included or not) has little effect on the lead compaction wave. This insensitivity is displayed in the $P - V$ Hugoniot diagram of Figure 5(a).

On the other hand, if we are interested in modeling the ignition of reaction in a granular bed, then the form we adopt for the solid EOS will play an important role. Predicting ignition, after all, is the goal of our program. In view of the order-of-magnitude argument given above, it is clear that the work associated with compaction of the bed,

$$\frac{P_s}{2\,\rho_s^0}\left(\frac{\phi_s}{\phi_s^0} - 1\right),$$

is typically substantially larger than the work associated with compression,

$$\frac{P_s}{2\,\rho_s^0}\left(1 - \frac{\rho_s^0}{\rho_s}\right).$$

Assuming that the work of compression is negligible, and that all the work associated with change of volume fraction goes to heat the solid, the increase in the solid temperature due to compaction would be

$$\Delta T_s = \frac{P_s}{2\,\rho_s^0\,C_{vs}}\left(\frac{\phi_s}{\phi_s^0} - 1\right) \ ,$$

which for granular HMX with $\phi_s^0 = 0.73$ and $\phi_s = 1$, yields

$$\frac{\Delta T_s}{P_s} = 93\ \mathrm{K/GPa}\ . \tag{43}$$

Of course, the work associated with change in porosity does not all go into heating. As discussed previously, in this model an amount of energy $B(\phi_s)$ is stored as recoverable compaction energy, so that at most only the portion

$$\frac{P_s}{2\rho_s}\left(\frac{\phi_s}{\phi_s^0} - 1\right) - B(\phi_s)$$

is available to heat the HMX. We call this dissipated energy compaction work. Figure 5(b) shows, on the $T - P$ Hugoniot diagram, the effect of including or ignoring B on heating. The ratio of compaction work to B as a function of ϕ_s is displayed in Figure 6, for two initial porosities ($\phi_s^0 = 0.65$ and $\phi_s^0 = 0.73$). Zero initially (*i.e.*, when $\phi_s = \phi_s^0$), the ratio increases with ϕ_s, becoming of the order of 2 or 3 when $\phi_s = 0.95$. For strong waves

(greater than 10 GPa pressure) the ratio is large, reflecting the fact that dissipative compaction work dominates the static compaction energy. On the other hand, for waves of about 0.5 GPa, B is a significant fraction of the compaction work, and our assumption of B as a reversible energy with no dissipation to thermalize the compaction energy leads to a lower temperature behind a compaction wave. One must emphasize, however, that the total compaction energy amounts to only 8.3 J/g for a 0.5 GPa wave, and based on the specific heat, can affect the temperature by about 9 K. Since at lower pressures the amount of energy available is small, undercounting of the heating due to the irreversibility is important, particularly when the compaction energy is localized in hot-spots as discussed below. The dissipation that occurs within a compaction wave is discussed further in Sec. (4.2).

As a further aid in understanding the role played by porosity in the heating of the solid grains, and the consequent enhancement of ignition sensitivity, we estimate the dependence of the time to explosion on shock strength and initial porosity. We use a simple Arrhenius rate law

$$\text{Rate} = (1-\lambda_s) Z \exp\left(-\frac{T^\ddagger}{T_s}\right),$$

where Z is the exponential prefactor and $T^\ddagger$ the activation temperature. The parameters for HMX are $Z = 5 \times 10^{19}\,\text{s}^{-1}$ and $T^\ddagger = 2.65 \times 10^4\,\text{K}$ [41]. For a given shock pressure P, the porosity is computed from $P = \phi_s \beta_s(\phi_s, \rho_s = \rho_s^0)$, the density ρ_s from the energy Hugoniot and temperature, T_s from the thermal EOS, all using Sheffield's calibration for HMX

$$\begin{aligned} P_s(\rho_s, e_{sp}) &= \frac{K_s^0}{N}\left\{\left(\left[\frac{\rho_s}{\rho_s^0}\right]^N - 1\right) - \frac{\Gamma_s^0}{N-1}\left(\left[\frac{\rho_s}{\rho_s^0}\right]^{N-1} - 1\right) + \Gamma_s^0\left(1 - \frac{\rho_s^0}{\rho_s}\right)\right\} \\ &\quad + \Gamma_s^0 \rho_s^0 \left[e_{sp} - e_{sp}^0 + C_{vs} T_s^0 \Gamma_s^0 \left(1 - \frac{\rho_s^0}{\rho_s}\right)\right] \qquad (44) \\ T_s(\rho_s, e_{sp}) &= T_s^0 + \frac{1}{\rho_s^0 C_{vs} \Gamma_s^0}\left\{P_s(\rho_s, e_{sp}) - \frac{K_s^0}{N}\left[\left(\frac{\rho_s}{\rho_s^0}\right)^N - 1\right]\right\}, \qquad (45) \end{aligned}$$

where $N = 10.3$. This EOS is reasonably accurate below about 10 GPa. The temperature is an estimate and was not measured.

The initial rate corresponding to T_s is plotted in Figure 7 as a function of shock pressure for both porous and full-density materials. The rate is very

sensitive to shock pressure, rising from 10^{-3} $(\mathrm{s})^{-1}$ at 2 GPa to $1\,(\mu\mathrm{s})^{-1}$ at 5 GPa for the porous solid. Prompt initiation will occur in the latter case. In contrast, even at 10 GPa the rate in full-density HMX is less than $1\,\mathrm{s}^{-1}$ and it would take some time for a detonation to develop, if it occurred at all. This is consistent with the observation that a single crystal of HMX does not detonate in 50 mm size samples when shocked to $O(\,10\,\mathrm{GPa})$ [42]. The vast difference in rate as porosity is varied is due to the exponential temperature dependence of the rate and variation of shock heating with porosity. Thus, granularity can have a dramatic affect on the chemistry.

The pressures achieved in a typical accident situation are of the order of (0.2 GPa). From Figure 5(b), the temperature rise behind a compaction wave in a porous bed is only about 15 K. This is an inconsequential increase in the bulk temperature. If the compaction work available to heat the bed can be deemed to be deposited near the surface of the grains, much as the "elastic" energy component of $B(\phi_s)$ is localized in small volumes around the contact surfaces of the grains, then the temperature increase would scale inversely with the fractional volume deemed to be associated with the compaction work. A fractional volume of 3% would lead to a local temperature increase of 450 K and an initial reaction rate of $0.2\,(\mu\mathrm{s})^{-1}$. A reaction rate of this magnitude corresponds to vigorous burning. A local region of high temperature is commonly referred to as a "hot-spot." If the "hot-spot" is large enough, then the energy generation due to reaction can exceed the conductive losses leading to significant localized reaction which in turn could build-up to a detonation wave. Some complications can occur with the simple bookkeeping described above. HMX is known to undergo a solid-to-solid phase transformation at 145 K above room temperature, which both consumes energy and results in a 10% volume increase in HMX. This can act to further load a confined granular bed. Also, melting occurs at 200 K above room temperature and the latent heat corresponds to a temperature change of 216 K. These may significantly affect the temperature and hence the rate estimated above.

A leading deficiency in the present model is that only bulk temperatures are included and temperature localization is ignored. However, at least qualitatively, the model does capture the physical source of the heating, namely, compaction work. The dissipated energy could be used to develop a rational "hot-spot" reaction mechanism. Although this mechanism is probably the dominant one for ignition in mechanical loading of granular beds at low pressures, we do not consider the question of these reaction centers in this work. Instead, we focus on examining the processes or exchange terms

that describe the dissipation that generates the heating; at least how they are mimicked in BN-type continuum mixture models for materials with microstructure, and how these exchange terms influence the equilibrium wave structures supported by the model.

Embid, Majda and Hunter [43] have proposed an alternative wave resonance theory for the generation of hot-spots, and imply that this could be the start of a deflagration-to-detonation transition. The theory is based on a singularity in the gas acoustic equations, noted by Embid and Baer[21], that occurs when the solid particle speed and either of the gas acoustic characteristics coalesce (*i.e.*, when $u_s = u_g \pm c_g$). Then the set of eigenvectors is not complete and the system of PDEs ceases to be hyperbolic. Given that the drag is large in low porosity systems, and therefore, the solid and gas particle speeds are nearly equal, this resonance is an unphysical artifact of the model, and unlikely to occur in any practical situation of interest. If the gas flow were sonic relative to the solid, the resulting drag force would increase enormously, leading to a rapid equilibration of the velocities. This effect was specifically excluded from the Embid-Majda-Hunter theory.

In the next section we re-examine how the dissipation inequality for the mixture can be used to define the exchange terms. We demonstrate that the dissipation inequality, when so applied, permits considerably more freedom in formulating the exchange terms than BN would imply.

3 The dissipation inequality

The BN model requires two types of constitutive input: (1) the EOSs for the equilibrium response of the separate components discussed in the last section, and (2) the source terms for rates of mass, momentum and energy exchange between phases, which is the subject of this section. Development of suitable models for both cases requires a blend of analysis and observation. While analysis provides constraints imposed by the principles of continuum mechanics, observations provide data for the specific material(s) at hand.

The methods for developing single-phase EOSs are rather standard and widely accepted. To a large extent, the EOS experiments can be carried out on large, well-controlled samples measuring response on a macroscopic scale to a limited number of well-understood control variables. However, obtaining a thermodynamically consistent EOS valid over a wide range may well be difficult.

Methods for measuring and parametrizing the exchange processes are not

nearly so well developed. In large measure this is a consequence of the short spatial and temporal scales on which these nonequilibrium processes can occur. For example, the resistance of a low-porosity granular bed to gas flow is typically measured by slow-flow experiments on macroscopic samples [44]. These measurements can only provide limited information about the high relative-speed flows that can occur over narrow, yet macroscopic (several grains), regions.

On the analytical side, the principal tool (besides material frame indifference and phase separation) is the dissipation (entropy) inequality for mixtures proposed by Truesdell [11],

$$(\eta_s - \eta_g)\,\mathcal{C} + (\phi_s \rho_s)\frac{d\eta_s}{dt_s} + (\phi_g \rho_g)\frac{d\eta_g}{dt_g} \geq 0\,, \tag{46}$$

where $d/dt_a = \partial_t + u_a \partial_x$ is the material derivative of an individual phase. Roughly the inequality implies that the entropy of an adiabatically insulated sample of a granular mixture cannot decrease spontaneously. Given that the temperature, pressure and velocity of each phase together with the volume fraction define the state of each phase, differences in the values of these variables could be viewed as the forces that drive changes in the state of the mixture.

3.1 Driving forces

To help motivate our choice of the set of driving forces, we first discuss the state of thermodynamic equilibrium for the mixture of granular solid and gas. This defines the relation between the pressure and temperature of the two phases when complete thermodynamic equilibrium is achieved. Sufficiently close to equilibrium, we can view compaction as reversible irrespective of whether we adopt the formulation $\Psi_s(\rho_s, T_s, \phi_s)$ (reversible) or $\Psi_s(\rho_s, T_s)$ (irreversible). In either case, β_s should be viewed as representing the reversible, elastic stress. We consider a nonreactive, quiescent (*i.e.*, $u_s = u_g = 0$), adiabatically closed system whose total internal energy, $e = \lambda_s e_s + \lambda_g e_g$, total volume, $V = \lambda_s/\rho_s + \lambda_g/\rho_g$ and mass fractions, (λ_s, λ_g) are constrained to remain constant. For such a mixture, the entropy of the system at equilibrium is a maximum with respect to all variations which leave e and V unchanged [45]. Using Eq. (27), the thermodynamic identity for the granular solid,

$$de_s = \frac{P_s}{\rho_s^2} d\rho_s + T_s\, d\eta_s + \frac{\beta_s}{\phi_s \rho_s} d\phi_s, \tag{47}$$

and the corresponding identity for the gas,

$$de_g = \frac{P_g}{\rho_g^2} d\rho_g + T_g d\eta_g, \tag{48}$$

the variation of mixture entropy (defined by Eq. (4)), near equilibrium and with e, V, λ_s and λ_g held constant, is

$$T_s d\eta = \frac{1}{\rho}(P_s - \beta_s - P_g) d\phi_s + \lambda_g (T_s - T_g) d\eta_g. \tag{49}$$

Since the variations $d\phi_s$ and $d\eta_g$ can be completely arbitrary, it follows that at equilibrium, the following conditions must both hold:

$$P_s - \beta_s - P_g = 0, \tag{50}$$

$$T_s - T_g = 0. \tag{51}$$

Equations (50–51) are the statements of pressure (mechanical) and temperature (thermal) equilibrium, respectively, for the granular mixture. Thus, we see that the configuration pressure represents the equilibrium pressure difference between the phases. With the definition of equilibrium at hand, we now put forth two postulates about the departure of the system from equilibrium. First, even when $T_s \neq T_g$, Eq. (50) will continue to define mechanical equilibrium. Likewise, Eq. (51) will remain our definition of thermal equilibrium even when $P_s - \beta_s - P_g \neq 0$. The second postulate pertains to the role of $(T_s - T_g)$ and $(P_s - \beta_s - P_g)$ as independent driving forces which serve as the agents that move the system from equilibrium. These forces are taken to be directly proportional to $P_s - \beta_s - P_g$ and $T_s - T_g$.

Similarly, we assume that the departure of $(u_s - u_g)$ from zero is proportional to a force that acts to cause interphase motion. The notion here is that Stokes-type drag is taken to be the corresponding restoring force. The forms of these driving forces are certainly consistent with total thermodynamic equilibrium, when the driving forces are zero. They are also plausible, and as we shall see, consistent with the notion that the dissipation inequality is linear in these forces for small departures from equilibrium.

A stable equilibrium for such a sample would require that dissipation be at least of second order in these differences at the equilibrium point. To ensure that the evolution is dissipative, source terms represented by the fluxes $\mathcal{M}$, $\mathcal{E}$ and $\mathcal{F}$ are chosen such that the entropy change for the mixture near equilibrium is the sum of positive-definite terms (in fact, perfect squares). Each term corresponds to a distinct physical process (drag, heat

conduction and compaction work) and these processes are required to be separately dissipative. This leads to relaxation-type expressions for the exchange rates which are consistent with equilibrium. This approach is reminiscent of that of Prigogine, who employed nonequilibrium thermodynamics to develop transport theories for simple mixtures [46].

Baer & Nunziato [12] imply that the exchange laws they derive in this way are in fact unique. Here we show that the general procedure allows considerably more flexibility in the forms for exchange laws. In particular, the entropy production for each physical process can be arbitrarily distributed between the phases. Consideration of the underlying physical process is needed to determine the free parameters in the constrained form of the source terms. In addition, when some exchange laws (such as the chemical conversion of solid to gas, and to a lesser extent, compaction) are known from experiment to be irreversible, and to have a particular dependence on the state variables, the entropy inequality can be used more creatively. Then, one can either place more constraints on the form of the exchange law or take the exchange rate as given, which would then serve to more tightly constrain the remaining exchange laws. We utilize this idea later in this section.

3.2 Nonreactive system

We demonstrate this procedure and the issue of nonuniqueness by first considering a simpler nonreactive model. The differential thermodynamic relation for either the solid phase, Eq. (27), or the gas phase (with $\beta_g = 0$) can be written as

$$T_a \, d\eta_a = de_a - \frac{P_a}{\rho_a^2} \, d\rho_a - \frac{\beta_a}{\rho_a \, \phi_a} \, d\phi_a \; . \tag{52}$$

On computing the material-specific time derivative and eliminating $d\rho_a/dt_a$ by means of the individual-phase mass conservation, Eqs. (7–8), one is led to the dissipation inequality for a nonreactive system,

$$\begin{aligned} &\frac{1}{T_s}\left[\phi_s\rho_s\,\left(\frac{de_s}{dt_s}+\frac{P_s}{\rho_s}\frac{\partial u_s}{\partial x}\right)+(P_s-\beta_s)\frac{d\phi_s}{dt_s}\right] \\ &\quad + \quad \frac{1}{T_g}\left[\phi_g\rho_g\,\left(\frac{de_g}{dt_g}+\frac{P_g}{\rho_g}\frac{\partial u_g}{\partial x}\right)+P_g\,\frac{d\phi_g}{dt_g}\right] \geq 0 \; . \end{aligned} \tag{53}$$

This expression assumes that the two-phase system is closed and locally adiabatic, *i.e.*, there is neither heat nor mass exchange with the surroundings.

Upon introducing source terms $\mathcal{M}$ and $\mathcal{E}$ into the single-phase momentum and energy equations (see Eqs. (9–12)), and then eliminating the kinetic energy from the latter, one finds that

$$\begin{aligned}\left(\frac{de_s}{dt_s} + \frac{P_s}{\rho_s}\frac{\partial u_s}{\partial x}\right) &= \frac{1}{\rho_s\,\phi_s}(\mathcal{E} - u_s\,\mathcal{M}) \\ \left(\frac{de_g}{dt_g} + \frac{P_g}{\rho_g}\frac{\partial u_g}{\partial x}\right) &= \frac{-1}{\rho_g\,\phi_g}(\mathcal{E} - u_g\,\mathcal{M})\;, \end{aligned} \tag{54}$$

where $\mathcal{E}$ and $\mathcal{M}$ denote the flux of energy and momentum, respectively, that flow through the interface separating the two phases. In the absence of all interphase exchange, $\mathcal{E} = \mathcal{M} = 0$. Then, neither phase gains or loses energy and momentum across the interfaces, and the components are said to be phase-isolated. Further, if no gasdynamic shocks are present, the changes in the overall entropy of the system,

$$\frac{1}{T_s}\,(P_s - \beta_s)\frac{d\phi_s}{dt_s} + \frac{1}{T_g}\,P_g\frac{d\phi_g}{dt_g}\;, \tag{55}$$

follow the changes in the volume fraction. On using $\phi_g = 1 - \phi_s$ and

$$\frac{d\phi_g}{dt_g} = -\frac{d\phi_s}{dt_s} + (u_s - u_g)\frac{\partial \phi_s}{\partial x}$$

(which assigns the porosity to the solid), the above expression is rewritten as

$$\left(\frac{P_s - \beta_s}{T_s} - \frac{P_g}{T_g}\right)\frac{d\phi_s}{dt_s} + \frac{P_g}{T_g}(u_s - u_g)\frac{\partial \phi_s}{\partial x}. \tag{56}$$

To reiterate: we have considered changes in system entropy for phases that are isolated both from each other and from their environment and interact only via changes in the volume fraction. Importantly, Eq. (56) can be of either sign, so that the entropy is not guaranteed to be nondecreasing.

When the system is in mechanical, temperature and velocity equilibrium (*i.e.*, $P_s = \beta_s + P_g$, $T_s = T_g$ and $u_s = u_g$), then changes in volume fraction produce no entropy [46]. In this limit, ϕ_s is not required in the modeling. The standard approach for modeling condensed phase explosives makes these assumptions [47].

To have the evolution of the system towards equilibrium reflect that the three forces

$$(P_s - \beta_s - P_g), \quad \left(\frac{1}{T_s} - \frac{1}{T_g}\right) \quad \text{and} \quad (u_s - u_g)$$

can act independently, it is necessary that momentum and energy flow across the phase interfaces. We now consider how the forms for the fluxes $\mathcal{M}$ and $\mathcal{E}$ can be constituted to reflect our choice of the driving forces in such a way that the dissipation inequality is satisfied.

We begin by recognizing that the decomposition

$$\left(\frac{z_s}{T_s} - \frac{z_g}{T_g}\right) = \left(\frac{1}{T_s} - \frac{1}{T_g}\right)\Big[z_s \cdot b + z_g \cdot (1-b)\Big] + (z_s - z_g)\left(\frac{1-b}{T_s} + \frac{b}{T_g}\right) \quad (57)$$

allows terms in the dissipation inequality to be expressed as the sum of terms proportional to the driving forces. By adjusting the parameter b between the limits $0 \leq b \leq 1$, the energy exchange due to compaction, say, can be partitioned either all to the solid ($b = 0$) or all to the gas ($b = 1$) or anywhere in between. We will take advantage of this ability later. Using Eq. (57), we can rewrite Eq. (56), to get

$$\begin{aligned} & \left(\frac{1}{T_s} - \frac{1}{T_g}\right)\Big[(P_s - \beta_s)\cdot b + P_g \cdot (1-b)\Big]\frac{d\phi_s}{dt_s} \\ + \quad & (P_s - \beta_s - P_g)\left(\frac{1-b}{T_s} + \frac{b}{T_g}\right)\frac{d\phi_s}{dt_s} + \frac{P_g}{T_g}(u_s - u_g)\frac{\partial \phi_s}{\partial x}. \end{aligned} \quad (58)$$

This regrouping of terms in Eq. (56) highlights the three agents that drive changes in the mixture entropy near equilibrium; the differences in temperature, pressure and velocity at the interface.

The source term involving $(u_s - u_g)$ is unlike the other terms. It can have either sign and unlike other sources, cannot be removed with a constitutive statement on $d\phi_s/dt_s$. More than any of the other terms, it motivates the inclusion of source terms in the momentum and energy equations to insure that dissipation inequality is satisfied. Substitution of Eqs. (54) into the dissipation inequality, Eq. (53), yields

$$\left(\frac{1}{T_s}-\frac{1}{T_g}\right)\mathcal{E}-\left(\frac{u_s}{T_s}-\frac{u_g}{T_g}\right)\mathcal{M}$$
$$\left(\frac{1}{T_s}-\frac{1}{T_g}\right)\left[(P_s-\beta_s)\cdot b+P_g\cdot(1-b)\right]\frac{d\phi_s}{dt_s}$$
$$+\quad (P_s-\beta_s-P_g)\left(\frac{1-b}{T_s}+\frac{b}{T_g}\right)\frac{d\phi_s}{dt_s}+\frac{P_g}{T_g}(u_s-u_g)\frac{\partial\phi_s}{\partial x}\geq 0\ . \quad (59)$$

We now employ Eq. (57) to rewrite Eq. (59), obtaining thereby an expression for the dissipation inequality in which terms are grouped according to the three driving forces,

$$\left(\frac{1}{T_s}-\frac{1}{T_g}\right)\left\{\mathcal{E} \quad - \quad \left[u_s\cdot w+u_g\cdot(1-w)\right]\mathcal{M}+\left[(P_s-\beta_s)\cdot b+P_g\cdot(1-b)\right]\mathcal{F}\right\}$$
$$+\quad (u_s-u_g)\left(\frac{1-w}{T_s}+\frac{w}{T_g}\right)\left\{\frac{P_g}{T_g}\frac{\partial\phi_s}{\partial x}\left(\frac{1-w}{T_s}+\frac{w}{T_g}\right)^{-1}-\mathcal{M}\right\}$$
$$+\quad (P_s-\beta_s-P_g)\left\{\left(\frac{1-b}{T_s}+\frac{b}{T_g}\right)\frac{d\phi_s}{dt_s}\right\}\geq 0\ . \quad (60)$$

The new parameters b and w are yet to be determined, though it seems natural to restrict $0\leq w\leq 1$ and $0\leq b\leq 1$ in order for the factors of temperature or pressure to interpolate between the values for the solid and gas phase. Defining the three terms in curly brackets to be $(T_g-T_s)\mathcal{H}$, $(u_s-u_g)\delta$ and

$$\frac{1}{\mu_c}\left(\frac{1-b}{T_s}+\frac{b}{T_g}\right)(P_s-\beta_s-P_g)\ ,$$

respectively, where $\mathcal{H}\geq 0$, $\delta\geq 0$ and $\mu_c>0$, ensures the positivity of each of the terms in the dissipation inequality. With this ansatz, the exchange terms are

$$\mathcal{M} = \frac{P_g}{T_g}\left(\frac{1-w}{T_s}+\frac{w}{T_g}\right)^{-1}\frac{\partial\phi_s}{\partial x}-\delta\,(u_s-u_g)\ , \quad (61)$$
$$\mathcal{E} = \mathcal{H}\cdot(T_g-T_s)$$
$$- \quad \left[(P_s-\beta_s)\cdot b+P_g\cdot(1-b)\right]\mathcal{F}+\left[u_s\cdot w+u_g\cdot(1-w)\right]\mathcal{M}\ , \quad (62)$$
$$\mathcal{F} = \frac{d\phi_s}{dt_s}=\frac{\phi_s\,\phi_g}{\mu_c}(P_s-\beta_s-P_g)\ . \quad (63)$$

These forms for the exchange laws reflect the fact that near equilibrium the exchanges are taken to be linear in the driving forces. We note that BN actually use the following alternate form for the compaction source,

$$\mathcal{F} = \begin{cases} \frac{\phi_s \phi_g}{\mu_c}\Big(P_s - \beta_s - P_g\Big)\,, & \text{for } P_s - \beta_s > 0; \\ -\frac{\phi_s \phi_g}{\mu_c}\, P_g\,, & \text{for } P_s - \beta_s \leq 0; \end{cases} \tag{64}$$

which is an attempt to model compaction as being irreversible. Since the signs of $\mathcal{F}$ and $P_s - \beta - P_g$ remain the same, the modified form is also consistent with the entropy inequality that we have presented in this section. The selection of the BN form over the equilibrium form given by Eq. (63) is an example of how independent information can be used along with the entropy inequality to deduce an improved form for an exchange term. In the next subsection we employ this idea more directly in treating reactivity.

We identify, as Baer and Nunziato did, $\mathcal{H}$ as a heat-transfer coefficient, δ as a drag coefficient and μ_c as a compaction viscosity. These are the quantities which, in concert with the prevailing levels of nonequilibrium, determine the rates of relaxation towards equilibrium. Their relative magnitudes, state-dependent in general, will determine the sequential order in which the system approaches velocity, mechanical and thermal equilibria. Since each process is separately dissipative, the coefficients $\mathcal{H}$, δ and μ_c may be determined and set independently. This allows the source terms to be calibrated and applied far from equilibrium.

The nonconservative term

$$P_N \frac{\partial \phi_s}{\partial x} \equiv \frac{P_g}{T_g}\left(\frac{1-w}{T_s} + \frac{w}{T_g}\right)^{-1} \frac{\partial \phi_s}{\partial x}$$

has already been identified as the nozzling term. In Appendix I we show that for the system of PDEs to be hyperbolic, $w = 1$. This implies that $P_N = P_g$, the BN value. Moreover, there is no entropy production in either phase associated with nozzling. It is worth reiterating that not all two-phase mixture models have a nozzling term. Eliminating nozzling by setting $P_N = 0$, as suggested by Powers *et al.* [16], puts the modeling PDEs in conservation form; a computational advantage. However, the entropy production for the mixture is not guaranteed to be positive semi-definite, though, in many applications, nozzling is small and the total entropy may well be non-decreasing. Here we follow the BN paradigm, for which nozzling contributes no entropy to the mixture.

With $b = w = 1$, we recover the BN exchange terms for a nonreactive system. However, the selection of a particular form for the parameters should either be based on a compelling physical argument or made with the realization that the choice is arbitrary. The parameter b is associated with distributing compaction work between the phases [48] and is discussed in more detail later in Sec. (4.2).

Finally, we note that even though BN assume $\Psi_s(\rho_s, T_s, \phi_s)$, which then implies the relation (see [21] Eq. (2.11))

$$T_s d\eta_s = de_s - \frac{P_s}{\rho_s^2} d\rho_s - \frac{\beta_s}{\phi_s \rho_s} d\phi_s,$$

they in fact use an EOS for the solid that does not depend on ϕ_s (see [21] Eq. (2.9), where $e_s(\rho_s, P_s)$). This is inconsistent. To remain true to the assumption $e_s(\rho_s, P_s)$ would require the standard single phase thermodynamic relation

$$T_s d\eta_s = de_s - \frac{P_s}{\rho_s^2} d\rho_s,$$

and would lead to some significant changes in the dissipation inequality. This in turn would have implications for the form of the compaction source $\mathcal{F}$. Importantly, if the compaction energy $B(\phi_s)$ is not accounted for then the configuration pressure, β_s would not appear naturally in the theory. We discuss some of these points later.

3.3 Reactive system

Progress was obtained relatively easily in the nonreactive case, $\mathcal{C} = 0$ because the issues were mostly mechanical and involved constitutive theory only via an EOS. In considering chemically reactive systems, we are forced to consider the very nonlinear constitutive functions typical of such processes. Also, instead of being symmetric as the "mechanical" processes were (*e.g.*, heat can flow both to and from the solid), we expect the chemistry to be one-sided, with $\mathcal{C} \leq 0$. Thus, we shall make a break with the traditional development here and include reactivity into the theory somewhat differently than the way in which we included the other processes. This apparent break from the development followed by BN is, in fact, in keeping with their approach, because BN never use the expression for $\mathcal{C}$ derived from a consideration of the entropy inequality.

On including chemistry (*i.e.*, mass transfer) in the elimination of $d\rho_a/dt_a$ from Eq. (52), the dissipation inequality for a nonreactive system, Eq. (53), is transformed into the reactive-system version

$$
\begin{aligned}
(\eta_s - \eta_g)\,\mathcal{C} \;&-\; \left(\frac{P_s}{T_s\,\rho_s} - \frac{P_g}{T_g\,\rho_g}\right)\mathcal{C} \\
&+\; \frac{1}{T_s}\left[\phi_s\rho_s\,\left(\frac{de_s}{dt_s} + \frac{P_s}{\rho_s}\frac{\partial u_s}{\partial x}\right) + (P_s - \beta_s)\frac{d\phi_s}{dt_s}\right] \\
&+\; \frac{1}{T_g}\left[\phi_g\rho_g\,\left(\frac{de_g}{dt_g} + \frac{P_g}{\rho_g}\frac{\partial u_g}{\partial x}\right) + P_g\,\frac{d\phi_g}{dt_g}\right] \geq 0\;. \qquad (65)
\end{aligned}
$$

As before, the momentum and energy exchange rates, $\mathcal{M}$ and $\mathcal{E}$, enter via the material-based rate of change of specific internal energy, given by

$$
\begin{aligned}
\left(\frac{de_s}{dt_s} + \frac{P_s}{\rho_s}\frac{\partial u_s}{\partial x}\right) &= \frac{1}{\rho_s\,\phi_s}(\mathcal{E} - u_s\,\mathcal{M}) - \frac{1}{\rho_s\,\phi_s}(e_s - \frac{1}{2}\,u_s^2\,)\,\mathcal{C}\;, \qquad (66)\\
\left(\frac{de_g}{dt_g} + \frac{P_g}{\rho_g}\frac{\partial u_g}{\partial x}\right) &= \frac{-1}{\rho_g\,\phi_g}(\mathcal{E} - u_g\,\mathcal{M}) + \frac{1}{\rho_g\,\phi_g}(e_g - \frac{1}{2}\,u_g^2\,)\,\mathcal{C}\;. \qquad (67)
\end{aligned}
$$

Following the discussion surrounding Eq. (21), we associate the compaction rate $\mathcal{F}$ with

$$
\frac{d\phi_s}{dt_s} - \frac{\mathcal{C}}{\rho_s} = \mathcal{F}\;.
$$

Substituting these expressions into Eq. (65) yields

$$
\begin{aligned}
\left(\frac{G_g}{T_g} - \frac{P_g}{\rho_s\,T_g} - \frac{G_s}{T_s} + \frac{P_s - \beta_s}{\rho_s\,T_s}\right)\mathcal{C} \;&+\; \frac{1}{2}\left(\frac{u_s^2}{T_s} - \frac{u_g^2}{T_g}\right)\mathcal{C} \\
+\left(\frac{1}{T_s} - \frac{1}{T_g}\right)\mathcal{E} - \left(\frac{u_s}{T_s} - \frac{u_g}{T_g}\right)\mathcal{M} \;&+\; \frac{P_g}{T_g}\,(u_s - u_g)\,\frac{\partial\phi_s}{\partial x} \\
&+\; \left(\frac{P_s - \beta_s}{T_s} - \frac{P_g}{T_g}\right)\mathcal{F} \geq 0\;, \qquad (68)
\end{aligned}
$$

where

$$
G_a \equiv \Psi_a + \frac{P_a}{\rho_a} = e_a + \frac{P_a}{\rho_a} - \eta_a\,T_a
$$

is the Gibbs free energy. We note that with the allowance for mass conversion, the Gibbs free energy now enters as an additional forcing term in the dissipation inequality.

In the limit of thermal equilibrium ($T = T_s = T_g$), velocity equilibrium ($u_s = u_g$) and mechanical equilibrium ($P_s = \beta_s + P_g$), porosity is an extraneous variable and $\mathcal{F}$, $\mathcal{M}$ and $\mathcal{E}$ play no role. Then the dissipation inequality is identical to the form for a homogeneous system

$$\left(\frac{G_g - G_s}{T}\right) \mathcal{C} \geq 0 \,. \tag{69}$$

In this case, it follows that the rate of mass conversion is in the direction to reduce the Gibbs free energy of the system; *i.e.*, $\mathcal{C} \leq 0$ when $G_s > G_g$. Typically, for explosives of interest, the change in the Gibbs free energy dominates the first term in Eq. (68) and the entropy inequality places no restriction on $\mathcal{C}$.

Here we assume that the mass conversion rate $\mathcal{C}$ is known, and show that the previously demonstrated flexibility in choosing the other exchange rates (*i.e.*, $\mathcal{M}$ and $\mathcal{E}$) is sufficient to insure that the mixture dissipation inequality can be satisfied. In doing this, we focus our attention on the first term in Eq. (68) proportional to $\mathcal{C}$, since it contains the new driving force. The second term in Eq. (68) presents no new problems since it can be lumped in with the coefficients of the three driving forces for the nonreactive problem discussed previously. The new modeling assumptions that are specific to a reactive mixture are:

(i) <u>entropy</u>: the entropy of the reacted gas is greater than that of the solid, *i.e.*, $(\eta_s - \eta_g) \leq 0$;

(ii) <u>irreversible reaction</u>: $\mathcal{C} < 0$;

The first term in Eq. (68) can be written as

$$\left(\frac{G_g}{T_g} - \frac{P_g}{\rho_s T_g} - \frac{G_s}{T_s} + \frac{P_s - \beta_s}{\rho_s T_s}\right) \mathcal{C} \;=\; \left(\frac{e_g + P_g\,(V_g - V_s)}{T_g} - \frac{e_s}{T_s}\right) C + \left[(\eta_s - \eta_g) - \frac{\beta_s}{\rho_s T_s}\right] \mathcal{C} \,. \tag{70}$$

By the assumptions above, the second term on the right hand is positive. Using Eq. (57), we can rewrite the factor in the first term on the right hand side as

$$\begin{aligned} \frac{e_g + P_g(V_g - V_s)}{T_g} \;-\; \frac{e_s}{T_s} &= \left(\frac{1-\nu}{T_s} + \frac{\nu}{T_g}\right) \Big[e_g - e_s + P_g(V_g - V_s)\Big] \\ &- \left(\frac{1}{T_s} - \frac{1}{T_g}\right) \Big[\nu e_s + (1-\nu)\Big(e_g + P_g(V_g - V_s)\Big)\Big] \,, \end{aligned}$$

where ν is an adjustable parameter chosen to satisfy the inequality

$$\left[e_g - e_s + P_g\,(V_g - V_s)\right]\left(\frac{1-\nu}{T_s} + \frac{\nu}{T_g}\right) \le \left[\eta_g - \eta_s + \frac{\beta_s}{\rho_s T_s}\right]. \qquad (71)$$

With ν selected so that Eq. (71) is satisfied, the contribution of the reactive term to the dissipation inequality is guaranteed to be positive. The choice of decompositions for the first reactive term in the dissipation inequality, Eq. (68), is somewhat arbitrary. Other rational choices are possible. The decomposition allows us to account for the remaining term proportional to the temperature difference in the source terms. Moreover, it reduces to the BN result when $\nu = 1$. Typically, $T_g > T_s$, $e_g - e_s + P_g\,(V_g - V_s) > 0$ and $\eta_g - \eta_s$ is the dominant term in inequality (71). In this case, the choice $\nu = 1$ is compatible with the principle of minimum entropy production for a non-equilibrium process when the temperature factor is assumed to interpolate between T_s and T_g.

We decompose the second reactive term in Eq. (68) according to

$$\begin{aligned}\frac{1}{2}\left(\frac{u_s^2}{T_s} - \frac{u_g^2}{T_g}\right)\mathcal{C} &= \frac{1}{2}\left(\frac{1}{T_s} - \frac{1}{T_g}\right)\left[u_s^2 f + u_g^2(1-f)\right]\mathcal{C} \\ &+ \frac{1}{2}(u_s - u_g)\,(u_s + u_g)\left(\frac{1-f}{T_s} + \frac{f}{T_g}\right)\mathcal{C}, \qquad (72)\end{aligned}$$

where f is a free parameter. The two forcing terms are proportional to differences in T and u as occurs in the nonreactive problem.

Grouping the terms in Eq. (68) according to the forces represented by the differences $\left(\frac{1}{T_s} - \frac{1}{T_g}\right)$, $(u_s - u_g)$ and $(P_s - \beta_s - P_g)$, the source terms can be chosen to form sums of squares, thus insuring positivity. The result is

$$\mathcal{M} = P_N\,\frac{\partial \phi_s}{\partial x} - \delta\,(u_s - u_g) + \frac{1}{2}\left(\frac{1-f}{T_s} + \frac{f}{T_g}\right) T_g\,(u_s + u_g)\,\mathcal{C}, \qquad (73)$$

$$\begin{aligned}\mathcal{E} &= \mathcal{H}(T_g - T_s) - P_c\,\mathcal{F} + u_s\,\mathcal{M} - \frac{1}{2}\left[u_s^2 f + u_g^2(1-f)\right]\mathcal{C} \\ &+ \left[\nu e_s + (1-\nu)\Big(e_g + P_g\,(V_g - V_s)\Big)\right]\mathcal{C}, \qquad (74)\end{aligned}$$

$$\mathcal{F} = \frac{d\phi_s}{dt_s} - \frac{\mathcal{C}}{\rho_s} = \frac{\phi_s\,\phi_g}{\mu_c}(P_s - \beta_s - P_g)\,, \qquad (75)$$

where

$$P_N = P_g \quad \text{and} \qquad P_c = (P_s - \beta_s)\,b + P_g(1-b). \qquad (76)$$

With $\nu = 1$, all the energy released by the reaction is deposited in the gaseous reaction products. Typically, when burning occurs $T_g > T_s$ and $e_g - e_s + P_g\,(V_g - V_s) > 0$. Then $\nu > 1$ corresponds to distributing some of the energy of the reaction to the solid phase reactants. In principle, this could be accounted for by heat conduction, *i.e.*, in the heat transfer coefficient $\mathcal{H}$. Similarly, $\nu < 1$ would withdraw additional energy from the solid and transfer it to the gas. This is possible when the reaction corresponds to a process such as evaporation but is not physically plausible for a highly exothermic irreversible reaction.

In addition to satisfying the entropy inequality the source terms must be compatible with Galilean invariance. The left-hand sides of the internal energy equations, Eqs. (66)-(67), are Galilean invariant. Therefore, the source term on the right hand side must be Galilean invariant as well. The terms involving the velocities are given by:

$$\begin{aligned} &\frac{1}{2}\,(u_s^2 - u_g^2)\,(1-f)\,\frac{\mathcal{C}}{\phi_s\rho_s}, && \text{for the solid;} \\ &\frac{T_g}{2\,T_s}\,(u_s^2 - u_g^2)\,(1-f)\,\frac{\mathcal{C}}{\phi_g\rho_g} - \frac{\delta}{\phi_g\rho_g}\,(u_s - u_g)^2, && \text{for the gas.} \end{aligned}$$

In both cases Galilean invariance requires $f = 1$.

3.4 Additional dissipation terms

There are two additional degrees of freedom related to the distribution of energy from drag. First, adding a term to the energy source,

$$\mathcal{E} \to \mathcal{E} + a\delta(u_g - u_s)^2,$$

changes the total dissipation due to drag from $\delta(u_s - u_g)^2/T_g$ to

$$\delta\left(\frac{a}{T_s} + \frac{1-a}{T_g}\right)(u_s - u_g)^2.$$

This is positive for $0 \le a \le 1$. The choice $a = 0$ in the BN-model corresponds to assigning all the dissipation from drag to the gas phase.

The second degree of freedom is related to the fact that the particle velocity changes when the material burns; *i.e.*, $u_s \to u_g$. Adding a drag term to the sources $\mathcal{M} \to \mathcal{M} - \alpha(u_g - u_s)\,\mathcal{C}$ and $\mathcal{E} \to \mathcal{E} - \frac{1}{2}\alpha(u_g + u_s)(u_g - u_s)\,\mathcal{C}$ increases the entropy production of the mixture by $-\frac{1}{2}\alpha\mathcal{C}(u_g - u_s)^2$. For

an irreversible reaction, $\alpha \geq 0$ would satisfy the entropy inequality and also is compatible with Galilean invariance. The choice $\alpha = 0$ in the BN-model minimizes the entropy increase due to drag when the material burns.

We now summarize the development of the interaction source terms.

(i) The dissipation inequality constrains but does not uniquely determine the source terms.

(ii) The physical requirements of Galilean invariance and a well posed initial value problem (hyperbolic system of PDEs) provides additional constraints ($w = 1$ and $f = 1$).

(iii) The remaining degrees of freedom must be determined based on application dependent considerations.

(iv) The BN model is recovered when $b = \nu = 1$ and $\alpha = 0$. Setting $\nu = 1$ gives a term e_s in the energy source term and seems natural for the energy balance equations. When the change in Gibbs free energy dominates the burn, the entropy inequality would not restrict ν. The parameter b is related to the distribution of compaction energy between the phases.

(v) When the solid-phase EOS is constituted as an EOS for a granular phase (*i.e.*, volume-fraction dependence is included), the configuration pressure β_s appears "naturally" in the compaction law. However, this formalism models quasistatic compaction as a reversible process. In order to reflect the irreversibility seen during the quasistatic compaction of HMX, additional variables and source terms will need to be introduced to model such processes as fracture, plastic deformation, and frictional heating. The entropy inequality will continue to be satisfied if these were separately dissipative, and each added a positive definite contribution to entropy production [49]. Such an approach is the subject of recent work by Gonthier *et al.*[34].

In the following sections, we show that the parameters are related to how the dissipation from each process is distributed between the phases. We suggest a number of expressions for the exchange terms that are physically more plausible than those used by BN.

4 Distribution of dissipation between phases: Modified interaction source terms

In their derivation of a two-phase model, Baer and Nunziato [12] used the entropy inequality to motivate the choice of the source terms for the interaction between phases. We have shown that many different choices are possible that satisfy the overall entropy inequality, and suggest the following modifications to the BN source terms:

$$\begin{aligned}\widetilde{\mathcal{E}} &= \mathcal{H}(T_g - T_s) + u_s\,\widetilde{\mathcal{M}} + a\delta(u_s - u_g)^2 \\ &\quad + \left\{-\frac{1}{2}u_s^2 + \nu e_s + (1-\nu)\left[e_g + P_g\left(V_g - V_s\right)\right]\right\}\mathcal{C}, \end{aligned} \tag{77}$$

where $0 \le a \le 1$ and ν satisfies Eq. (71), and

$$P_c = (P_s - \beta_s)b + P_g(1-b), \qquad 0 \le b \le 1. \tag{78}$$

In this section, we argue on physical grounds for reasonable choices for the parameters a, b and ν. For this purpose, its helpful to record the individual phase energy and entropy equations, where we have taken $f = w = 1$ in Eqs. (66)-(67). We get for the solid,

$$\begin{aligned}\phi_s\,\rho_s\left(\frac{de_s}{dt_s} + P_s\frac{dV_s}{dt_s}\right) &= \mathcal{H}(T_g - T_s) + \beta_s\mathcal{F} + (1-b)(P_s - \beta_s - P_g)\mathcal{F} \\ &+ a\,\delta(u_s - u_g)^2 - (1-\nu)\Big[e_s - e_g - P_g(V_g - V_s)\Big]\,\mathcal{C} \\ &= \phi_s\rho_s T_s\frac{d\eta_s}{dt_s} + \beta_s\frac{d\phi_s}{dt_s}, \end{aligned} \tag{79}$$

where we have used Eq. (27), and for the gas

$$\begin{aligned}\phi_g\,\rho_g\left(\frac{de_g}{dt_g} + P_g\frac{dV_g}{dt_g}\right) &= -\mathcal{H}(T_g - T_s) + b(P_s - \beta_s - P_g)\,\mathcal{F} \\ &+ (1-a)\,\delta(u_s - u_g)^2 - \nu\Big[e_s - e_g - P_g(V_g - V_s)\Big]\,\mathcal{C} \\ &= \phi_g\,\rho_g\,T_g\frac{d\eta_g}{dt_g}. \end{aligned} \tag{80}$$

We have rewritten the left-hand side of each individual-phase energy equation so as to highlight the material-based, isolated-phase, first-law form of

the equation. This has the effect of moving the compaction-related part of $\partial u_a/\partial x$ to the right hand side as a source term. Thus, the apportioning of dissipation between phases is controlled for drag by a, for compaction by b, and for burn by ν. Also, Eqs. (79)–(80) exhibit the property of the model that quasistatic compaction (*i.e.*, $P_s = \beta_s + P_g$) does not generate any entropy in either phase, which is a consequence of our thermodynamic description of $B(\phi_s)$ as a potential energy.

The assumption that the solid has a stiff EOS relative to the gas leads to the formulation of an advection equation for compaction dynamics, Eq. (21), along solid particle trajectories. Consistent with this idea is the consignment of the entire drag dissipation to the gas. Thus, at low pressures when the compaction dynamics is physically reasonable, the choice $a = 0$ is appropriate. At higher pressures the drag is not significant compared to other dissipative processes, in particular burn, so the partition for drag is unimportant there.

Usually the empirical form used for the reaction rate is taken to be a strong function of gas pressure once the ignition criteria for the reaction is exceeded. Thus, at low pressures taking $\nu = 1$ and sending the reaction energy to the gas would magnify the reactive response of the granular bed. As the pressures increase and $P_s \approx P_g$, the reactive response would be insensitive to the value of ν.

In actual fact, the forms presented for the exchange terms should be thought of as a first guess. More information on the microstructural physics needs to be developed to constitute the continuum-scale exchange terms used in such theories as BN with improved realism. Nevertheless, if physically plausible exchange terms of the sort we have derived are used intelligently, we should be able to explore whether the phenomena observed in experiments on granular explosives can be sensibly mimicked by multiphase continuum mixture models such as a modified-BN. Using such modified source terms, we now show how inconsistencies in the BN-model related to compaction work and the single-phase limit can be corrected by appropriately modifying the source terms.

4.1 Compaction work

Here we discuss the dissipative terms associated with compaction in this theory called "compaction work". These dissipative terms contribute compaction related energy to the mixture in addition to the previously discussed contribution to the energy of a granular solid, $B(\phi_s)$. We argued that $B(\phi_s)$

represented an energy that was localized near the contact surfaces of the solid grains. This compaction energy, discussed in Sec. (2.5), is measured in the quasistatic compaction experiments of Elban & Chiarito [36] in which a granular material within a cylinder is slowly compressed by a piston. The "compaction work" terms play no role there; being associated with a dynamic process, they play a role only in dynamic compaction experiments, and in general lead to a rate dependence of the achieved end state.

Recall that compaction dynamics involves terms proportional to $\mathcal{F}$. In the original BN-model, where $b = 1$, the compaction process is dissipative for the gas phase since the entropy change of the gas is given by

$$(P_s - \beta_s - P_g)\mathcal{F} \propto (P_s - \beta_s - P_g)^2 \geq 0 \ ,$$

whereas the entropy change for the solid is zero. Our modification to the exchange terms includes a parameter $0 \leq b \leq 1$. It allows us to distribute the compaction work between the phases in any fashion, with the contribution to both the solid and gas entropy equations, Eqs. (79)-(80), being positive

$$\begin{aligned} (1-b)(P_s - \beta_s - P_g)\mathcal{F} &\geq 0, \qquad \text{for solid,} \\ b(P_s - \beta_s - P_g)\mathcal{F} &\geq 0, \qquad \text{for gas.} \end{aligned}$$

The term $b(P_s - \beta_s - P_g)\mathcal{F}$, which appears with equal magnitude but opposite sign in the individual phase equations, sets the partition of the energy of compaction between the solid and the gas. This is a similar functionality to the drag terms that we considered earlier. When b takes on the BN value of 1, the gas would gain the maximum amount of energy allowed during compaction, while <u>none</u> of the compaction energy would go to the gas when $b = 0$. The term $\beta_s\mathcal{F}$ on the right hand side of Eq. (79) consistently represents the increase in the quasistatic compaction energy of the solid and $(P_s - \beta_s - P_g)\mathcal{F}$ represents the increase in the internal energy of the solid due to compaction work, as we now show.

We integrate the solid energy equation, Eq. (79), under the following assumptions: (i) $\rho_s = \rho_s^0$, because as we discussed in Sec. (2.5) the density of the solid phase does not change much on compaction. (ii) Compaction provides sufficient dissipation to lead to a fully dispersed steady traveling wave profile. (iii) With a negligible gas mass fraction, $P_g \approx 0$. Then for a compaction wave we obtain

$$\triangle e_s \approx \int_1^2 \frac{dB(\phi_s)}{d\phi_s}\, d\phi_s + \int_1^2 \frac{(1-b)(P_s - \beta_s)\mathcal{F}}{\rho_s^0\, \phi_s}\, dt_s \ , \tag{81}$$

where the subscripts 1 and 2 denote the initial and final compaction states. The first term on the right hand side in Eq. (81) is the quasistatic compaction energy from the intergranular stress, denoted B in Eq. (33). The second term is the dissipative compaction work due to the dynamic compaction process. The sum of the two terms is determined by the Hugoniot jump relation, Eq. (41) given in Sec. (2.5)

$$\triangle e_s \approx \frac{P_s}{2\ \rho_s^0} \left(\frac{\phi_s}{\phi_s^0} - 1 \right) \ ,$$

where we have taken $\rho_s \approx \rho_s^0$. As we showed in Sec. (2.5), the quasistatic compaction energy is a third of the dissipative compaction work when material initially at $\phi_s^0 = 0.65$ is dynamically compressed to 5% porosity.

The parameter b distributes the compaction dissipation between the solid and gas phases. The choice $b = 1$ in the original BN-model corresponds to all the compaction dissipation occurring in the gas. In this case, when the gas mass fraction is small (as occurs for the lead compaction wave in a DDT tube experiment), attributing all the dissipation to the gas leads to an unphysically high gas temperature, much higher than the temperature behind a detonation wave. This is because the fixed energy from compaction is placed into an arbitrarily small mass of gas, as we show in the next subsection.

A better choice for the parameter is $b = 0$. This corresponds to attributing the compaction dissipation to the solid. As the next subsection also shows, this choice is needed to obtain fully dispersed weak compaction waves. Alternatively, $b = \lambda_g$ or P_g/P would distribute the dissipative compaction work between the solid and gas in a physically plausible manner.

4.2 Single-phase limit

As the mass fraction of the gas becomes vanishingly small, it is natural to expect that the influence of the gas on the behavior of the system should decline accordingly, and in the limit the model should reduce to that for a gasless porous solid. We now explore whether this single-phase limit is achieved in a consistent way.

In order to derive the limit, we start with the assumption that the gas has a small mass fraction, *i.e.*,

$$\phi_g \rho_g << \phi_s \rho_s. \tag{82}$$

Below crush-up the porosity may be moderate and then the above condition holds because the gas is far less dense than the solid ($\rho_g << \rho_s$). Above crush-up the porosity is small, $\phi_g << 1$, causing the above condition to be satisfied even when the gas has been compressed to a density comparable to that of the solid ($\rho_g = O(\rho_s)$). We also assume that the velocities $u_s,\ u_g$ and the specific internal energies $e_s,\ e_g$ are of order unity. Since p_a/ρ_a is a measure of e_a, the condition on the internal energies implies that $p_a = O(\rho_a)$ for both phases as well. It then follows that

$$\phi_g P_g << \phi_s P_s \qquad \text{and} \qquad \phi_g \rho_g u_g << \phi_s \rho_s u_s. \tag{83}$$

For the mixture variables, Eqs. (82) and (83) imply that

$$\begin{aligned} \rho \equiv \phi_s \rho_s + \phi_g \rho_g &\approx \phi_s \rho_s, \\ P \equiv \phi_s P_s + \phi_g P g &\approx \phi_s P_s, \\ e \equiv (\phi_s \rho_s e_s + \phi_g \rho_g e_g)/\rho &\approx e_s, \\ u \equiv (\phi_s \rho_s u_s + \phi_g \rho_g u_g)/\rho &\approx u_s. \end{aligned}$$

As a result, the gas contributions can be neglected in the mixture equations for the conservation of mass, momentum and energy (obtained by adding together respective contributions from each phase in Eqs. (7)-(12)), reducing them to the standard, single-phase fluid equations,

$$\begin{aligned} \frac{\partial \rho}{\partial t} + \frac{\partial \rho u}{\partial x} &= 0, \\ \frac{\partial (\rho u)}{\partial t} + \frac{\partial (\rho u^2 + P)}{\partial x} &= 0, \qquad (84) \\ \frac{\partial (\rho E)}{\partial t} + \frac{\partial [(\rho E + P)\, u]}{\partial x} &= 0, \\ \frac{\partial \phi_s}{\partial t} + u \frac{\partial \phi_s}{\partial x} &= \mathcal{F}. \qquad (85) \end{aligned}$$

Although derived above from the conservation laws for the mixture, Eqs. (84) are simply the balance laws for the solid phase alone, with the exchange terms removed. For consistency, therefore, the exchange terms in the solid-phase equations themselves must vanish in the single-phase limit. In order to ensure the satisfaction of this requirement, we examine the momentum and energy exchange processes in turn.

It is natural to take the mass exchange rate $\mathcal{C} = 0$ in the single phase limit; otherwise, the gas mass fraction will not stay small. In the momentum

exchange term $\mathcal{M}$, the only contributions that remain in the absence of chemistry are those due to nozzling and drag, so that the solid momentum equation (9) reduces to

$$\frac{\partial}{\partial t}\left(\phi_s \rho_s u_s\right) + \frac{\partial}{\partial x}\left(\phi_s \rho_s u_s^2 + \phi_s P_s\right) = \delta(u_g - u_s) - P_g \frac{\partial \phi_g}{\partial x}.$$

The aforementioned consistency requirement forces the nozzling and drag combination on the right-hand side to be vanishingly small. Now the nozzling term limits to zero either because $P_g << 1$ or because $\phi_g << 1$. The drag term $\delta(u_s - u_g)$ must then also vanish on its own, *i.e.*,

$$\delta(u_s - u_g) << 1.$$

In order to assess the consistency of the energetics in the single-phase limit, we turn to the solid energy equation (11). With mass exchange $\mathcal{C}$ set to zero and drag neglected, this equation reads

$$\begin{aligned} \frac{\partial}{\partial t}\left\{\phi_s \rho_s \left(e_s + \frac{1}{2}u_s^2\right)\right\} \quad &+ \quad \frac{\partial}{\partial x}\left[\phi_s u_s \left\{\rho_s \left(e_s + \frac{1}{2}u_s^2\right)\right\} + P_s)\right] \\ &= \quad -P_g u_s \frac{\partial \phi_g}{\partial x} - [b(P_s - \beta_s) + (1-b)P_g]\mathcal{F}. \end{aligned}$$

Here we have ignored heat transfer between the phases as well, to ensure that the single-phase limit exists even in the worst case, when the gas is unable to transfer any heat back to the solid. As argued above, the nozzling term on the right-hand side of the above equation is negligible, so that the compaction term must be vanishingly small on its own. Below crush-up, when P_g is small but ϕ_g (and hence $\mathcal{F}$) can be moderate, this requires that the partition coefficient b must be set to zero. Above crush-up, the compaction term is negligible because porosity (and hence $\mathcal{F}$) is small.

To complete the argument we examine the entropy form of the gas energy equation

$$\phi_g \rho_g \Big(\frac{de_g}{dt} - \frac{P_g}{\rho_g^2}\frac{d\rho_g}{dt}\Big) = b(P_s - \beta_s - P_g)\mathcal{F},$$

obtained from Eq. (80), where once again the chemical, drag and heat-transfer contributions have been neglected. The left-hand side vanishes in the limit, and the selection $b = 0$ made above causes the right-hand side to vanish as well.

Thus we see that the one-phase limit is consistently attained. Additionally, the deposition of all compaction work into the solid provides a natural

dissipation mechanism for weak compaction waves to be fully dispersed, a phenomenon observed in practice. The above analysis corrects a deficiency in the BN – model which, having made the choice $b = 1$ and thereby assigning all compaction work to the gas, is unable to limit properly.

5 Final remarks

Modeling the behavior of damaged explosives and propellants is important for safety studies. The wide disparity between the particulate scale of the damaged material and the scale of the device would make a micromechanical model impractical. Additionally, reproducibility of DDT experiments on granular HMX implies a well-behaved response, in the sense that the "averaged" behavior is insensitive to variations in the microstructure that occur from experiment to experiment. These observations argue for a continuum model, one that would employ a two-phase framework to account for the solid grains of the explosive and the gaseous products of combustion.

Various versions of a two-phase, continuum theory of DDT have been proposed. Among the latest, and more prominent, examples of this approach is the Baer-Nunziato model [12]. This model has been tested by comparing its computational results to experimental observations from DDT tube experiments with granular explosives. Appropriately calibrated, the model can reproduce quite well a subset of the available experimental observations, but not all of the impact data as the projectile velocity varies [9, 8]. To evaluate accident scenarios it is important for a model to apply over the wide range of conditions that may occur.

In this paper we have critically examined the continuum-mechanical underpinnings of the BN model; both the stated physical approximations and the tacit assumptions upon which it is based. Given the complexity of the physical problem being modeled, such an examination is absolutely vital so that the strengths of the model, as well as its limitations, are clearly identified and understood before any extensions are undertaken or generalizations attempted to broaden its range of validity.

The BN model requires constitutive information on two levels: 1) an EOS for each of its two constituents, and 2) rate expressions for the exchange terms that act across the particulate/gas interfaces. We have reexamined the formulation of the material-specific constitutive terms and identified their physical basis; a feature not present in the original derivation. Inconsistencies in the EOS for the granular solid have been corrected.

BN relies heavily on the dissipation inequality for the development of constitutive expressions for the interfacial exchange rates. We demonstrate that this inequality allows considerably more flexibility in constraining the interphase exchange terms than has been suggested by BN. We identify and exploit this flexibility to construct physically improved exchange terms. These improvements allow one to remove inconsistencies from the original formulation, especially those connected to single-phase limits and subsonic dispersed compaction waves. Both require that the dissipative compaction work be apportioned to the solid phase rather than the gas phase as in the original model.

In order to extend the domain of applicability of the model and to increase its utility as a tool for safety predictions, several improvements remain to be made. The present formalism, wherein the solid-phase internal energy has a volume-fraction dependent component, treats the compaction energy as a potential and hence, quasistatic compaction as reversible. Further work, along the lines indicated by Gonthier *et al.* [34], is needed to capture the observed irreversible aspects of slow compaction. With the simple constitutive model of compaction energetics and configuration stress, the fluid-like BN model, as it stands, can describe subsonic compaction waves and DDT. To have an extended validity in some multidimensional situations, the model will need to be extended to treat other properties dependent on the material strength of the grains, such as mesoscale shear.

Burn models, at the moment, are the weakest feature of the theory. Sufficiently strong compaction waves lead to hot spots, *i.e.*, regions where energy is localized. Owing to the sensitivity of the reaction to temperature, these hot spots are the sites of ignition, and dominate the rate of combustion prior to the onset of detonation. Ignition at hot spots depends most strongly on the size and temperature of the hot-spot itself, and not on the bulk temperatures that appear in the continuum theory. While the (experimentally derived) compaction work describes the net energy available for ignition, the theory is silent on how this energy is partitioned (localized). It needs constitutive information, from experiments and possibly, detailed micromechanical calculations, about the phenomenon of localization and about the way it initiates ignition. Additional degrees of freedom are required in BN to treat such issues. Without such a feature, DDT models are not likely to be applicable over a sufficiently wide range of conditions.

The model, in its present form, is designed to deal only with a granular material that is well-characterized. What variables are needed to characterize damage in an explosive remains an important but open question that

must be addressed successfully if the model is to be used for engineering studies of explosive safety.

Whatever constitutive expressions are in place, they contain within them information about the length and time scales of the underlying microstructure. These scales, in turn, determine the spatial and temporal extents of the zones in which the exchange processes strive to move the system towards equilibrium. Accuracy requires that in a numerical computation, these zones be adequately resolved. If their characteristic scales are thin compared to the physical dimensions of the system being examined, the associated computational burden could be prohibitively excessive. Such a situation is ripe for exploring asymptotic reductions of the model, in which the thin zones would be shock-like discontinuities that need not be resolved, and across which appropriate variables would undergo predetermined jumps. For example, experiments on permeation [44] as well as numerical simulations with the BN model [48] show that at low porosity (relevant to the situation at hand) the drag is high, $\delta \approx 200\,\mathrm{kg}/(\mathrm{m}^3 \cdot \mu\mathrm{s})$, and the time scale for velocity equilibration is thus short,

$$\tau_u \sim \phi_g \rho_g / \delta = 0.1\,\mu\mathrm{s}\ ,$$

leading to a length scale for velocity equilibration based on the solid sound speed, c_s of $\tau_u c_s \sim 0.3\,\mathrm{mm}$. This scale is comparable to the grain size, and thus very small relative to the scales at which the continuum model holds. Thus, over major portions of the DDT event, carrying two velocity variables is an unnecessary complication because the source terms associated with drag are stiff. In addition, the two velocities lead to difficulties at the interface with a nonporous inert material which has only one velocity. (Witness the pressure oscillations at the interface in figure 5 of [50], where BN-based computations of impact experiments are reported.) This suggests a natural reduction of the model, over a significant portion of the DDT event, to one which carries only one velocity to a first approximation. At pressures above the yield strength of the explosive grains the length scale for pressure equilibration is found to be small as well, thus motivating a further reduction to a single pressure. These reduced models, economical from both analytical and computational viewpoints, are derived [2] and studied [3] in two forthcoming papers in this series.

Acknowledgments

We thank Larry Hill of Los Alamos for helpful discussions and Don Drew and Steve Passman for sharing with us a manuscript of their book (in preparation) on continuum mixture theory. This work has been supported by the United States Department of Energy, under contract W-7405-ENG-36. AKK was also supported partially by the National Science Foundation.

Appendix I: Hyperbolicity

The modified source terms derived in Sec. (3.2) can affect the mathematical structure of the modeling PDEs. Given our postulate that the modeling PDEs should be evolutionary (hyperbolic), in this appendix we examine whether the modifications to the nozzling term (*i.e.*, allowing $w \neq 1$) can lead to PDEs that are not hyperbolic. To simplify the analysis, we use P, u and η as the dependent variables for each phase and set all algebraic source terms (such as heat transfer, drag, compaction and chemical reaction) to zero.

The evolution equations for the solid and gas phase entropy are

$$\phi_s \rho_s T_s \frac{d\eta_s}{dt_s} + (1-w)(u_s - u_g) P_N \frac{\partial \phi_s}{\partial x} = 0 \,, \tag{86}$$

$$\phi_g \, \rho_g \, T_g \frac{d\eta_g}{dt_g} - (1-w)(u_s - u_g) P_N \frac{\partial \phi_s}{\partial x} = 0 \,. \tag{87}$$

The solid and gas mass equations can be put in a more convenient form by eliminating V_a using the thermodynamic identities

$$\begin{aligned} V_s \, dP_s &= -\gamma_s P_s \, dV_s + \Gamma_s T_s \, d\eta_s \,, \\ V_g \, dP_g &= -\gamma_g P_g \, dV_g + \Gamma_g T_g \, d\eta_g \,, \end{aligned}$$

where Γ_a is the Gruneisen parameter. In deriving these identities we have used the definition of the adiabatic exponent

$$\gamma_a = -\left(\frac{\partial \ln P_a}{\partial \ln \rho_a} \right)_{\eta_a, \phi_a} = \frac{\rho_a c_a^2}{P_a} \,,$$

where c_a is the sound speed. The source-free solid and gas phase mass equations thus become

$$\phi_s \frac{dP_s}{dt_s} \quad + \quad \phi_s \rho_s c_s^2 \frac{\partial u_s}{\partial x} - \Gamma_s \phi_s \rho_s T_s \frac{d\eta_s}{dt_s} = 0 \,, \tag{88}$$

$$\phi_g \frac{dP_g}{dt_g} \quad + \quad \phi_g \rho_g c_g^2 \frac{\partial u_g}{\partial x} - \Gamma_g \phi_g \rho_g T_g \frac{d\eta_g}{dt_g} + \rho_g c_g^2 (u_s - u_g) \frac{\partial \phi_s}{\partial x} = 0 \ . \quad (89)$$

The source-free solid and gas momentum equations can be written

$$\phi_s c_s \frac{\partial P_s}{\partial x} \quad + \quad \phi_s \rho_s c_s \frac{du_s}{dt_s} + (P_s - P_N) c_s \frac{\partial \phi_s}{\partial x} = 0 \ , \quad (90)$$

$$\phi_g c_g \frac{\partial P_g}{\partial x} \quad + \quad \phi_g \rho_g c_g \frac{du_g}{dt_g} - (P_g - P_N) c_g \frac{\partial \phi_s}{\partial x} = 0 \ . \quad (91)$$

This system of PDEs, Eqs. (86-91) plus Eq. (21), can be written as a matrix equation

$$\mathbf{H}\, \partial_t \vec{q} + \mathbf{F}\, \partial_x \vec{q} = \text{source} \ ,$$

where

$$\vec{q}^{\top} = (\vec{q}_s^{\top}, \, \phi_s, \, \vec{q}_g^{\top}) \ , \quad (92)$$

and the single phase variables are $\vec{q}_a^{\top} = (P_a, \, u_a, \, \eta_a)$. By taking linear combinations of the rows we find

$$\widetilde{\mathbf{F}} \equiv \mathbf{H^{-1}F} = \begin{pmatrix} \widetilde{\mathbf{F}}_s & \vec{S} & \mathbf{0} \\ \vec{0}^{\top} & u_s & \vec{0}^{\top} \\ \mathbf{0} & \vec{G} & \widetilde{\mathbf{F}}_g \end{pmatrix} \ , \quad (93)$$

where $\widetilde{\mathbf{F}}_a$ is the flux matrix for the single phase fluid equations

$$\widetilde{\mathbf{F}}_a = \begin{pmatrix} u_a & \rho_a \, c_a^2 & 0 \\ V_a & u_a & 0 \\ 0 & 0 & u_a \end{pmatrix} \ , \quad (94)$$

and the coupling of the phases with the volume fraction is given by the vectors

$$\vec{S} = \left(\frac{\Gamma_s (1-w) P_N}{\phi_s} (u_s - u_g), \quad \frac{P_s - P_N}{\phi_s \rho_s}, \quad \frac{(u_s - u_g)(1-w) P_N}{\phi_s \rho_s T_s} \right)^{\top} ,$$

$$\vec{G} = \left(-\frac{[\Gamma_g (1-w) \frac{T_g}{T_s} P_N - \rho_g c_g^2]}{\phi_g} (u_s - u_g), \quad \frac{P_N - P_g}{\phi_g \rho_g}, \quad -\frac{(u_s - u_g)(1-w) P_N}{\phi_g \rho_g T_s} \right)^{\top} .$$

The simple form of the matrix $\widetilde{\mathbf{F}}$ allow the eigenvalues and eigenvectors to be calculated analytically. The characteristic velocities are simply those for the solid phase $u_s - c_s$, u_s, $u_s + c_s$, the gas phase $u_g - c_g$, u_g, $u_g + c_g$,

and an additional characteristic velocity u_s from the compaction dynamics equation.

We note that the characteristic velocity u_s is two-fold degenerate. For the BN model (*i.e.*, $w = 1$) this does not lead to any problems since the right eigenvectors are found to be complete (except at isolated surfaces in the state space). The situation is different for the modified BN-model. The above analysis shows that the modified nozzling terms can lead to the model not being hyperbolic. We investigate this point next.

The right eigenvector corresponding to the degenerate eigenvalue u_s requires special consideration. Let the components of the eigenvector be denoted by q_i. The third component of the eigenvalue equation $\widetilde{\mathbf{F}}\vec{q} = u_s\vec{q}$ is

$$u_s q_3 + \frac{(u_s - u_g)(1-w)P_N}{\phi_s \rho_s T_s} q_4 = u_s q_3 \ .$$

This implies that $q_4 = 0$ unless either $w = 1$, $P_N = 0$ (no nozzling) or $u_s = u_g$ (single velocity). If $q_4 = 0$ then there is only one right eigenvector, (0, 0, 1, 0, 0, 0, 0), corresponding to the two-fold degenerate eigenvalue u_s. A second linearly independent eigenvector for the two-fold degenerate eigenvalue u_s can be found in terms of a time dependent solution of the form

$$(b_1,\, b_2,\, t,\, b_4,\, b_5,\, b_6,\, b_7) \ , \tag{95}$$

where b_i are calculable constants. However, the t-dependence in Eq. (95) renders the associated linearized problem ill-posed [51]. Any initial data that selects this right-eigenvector would lead to an unbounded, linear growth of the solution with time.

If $w = 1$, then the additional right eigenvector is $\left(\frac{P_N - P_s}{\phi_s},\, 0,\, 0,\, 1,\, 0,\, 0,\, 0\right)$. Hence, for the two-phase model equations to be hyperbolic we require $w = 1$. Thus, $P_N = P_g$ and the velocity associated with the nozzling in the energy source term must be the solid particle velocity used to convect the volume fraction. As a consequence, nozzling does not contribute to the dissipation of either the solid or the gas phase. Since the Hugoniot jump equations are compatible with ϕ_s continuous across a shock [21], the non-conservative nozzling term, $\partial\phi_s/\partial x$, does not cause a problem for the wave structure.

References

[1] A. K. Kapila, S. F. Son, J. B. Bdzil, R. Menikoff, and D. S. Stewart. Two-phase modelling of DDT: Structure of the velocity-relaxation zone. *Phys. Fluids*, 9[12]:3885–3897, 1997.

[2] A. K. Kapila, J. B. Bdzil, R. Menikoff, S. F. Son, and D. S. Stewart. Two-phase modelling of DDT: Reduced models derivation. *in preparation*, 1997.

[3] S. F. Son, J. B. Bdzil, R. Menikoff, A. K. Kapila, and D. S. Stewart. Two-phase modelling of DDT: Reduced models and numerical simulations. *in preparation*, 1997.

[4] H. W. Sandusky and R. R. Bernecker. Compressive reaction in porous beds of energetic materials. In *Eighth International Symposium on Detonation*, pages 881–891, 1985.

[5] J. M. McAfee, B. Asay, W. Campbell, and J. B. Ramsay. Deflagration to detonation in granular HMX. In *Ninth (International) Symposium on Detonation, Portland, OR, Aug. 28, 1989*, pages 265–279, 1989.

[6] A. F. Belyaev, V. K. Bobolev, A. I. Korotkov, A. A. Sulimov, and S. V. Chuiko. *Transition from Deflagration to Detonation in Condensed Phases*. Keter Publishing House Jerusalem Ltd. (available from the US Department of Commerce), 1975.

[7] P. E. Luebcke, P. M. Dickson, and J. E. Field. An experimental study of the deflagration-to-detonation transition in granular secondary explosives. *Proc. R. Soc. Lond. A*, 448:439–448, 1995.

[8] E. Kober, J. B. Bdzil, and S. F. Son. Modeling DDT in granular explosives with a multidimensional hydrocode. In *APS Topical Conference of Shock Compression in Condensed Matter - 1995, Proceedings of the American Physical Society Topical Conference, Seattle, WA*, pages 437–441, 1996.

[9] S. A. Sheffield, R. L. Gustavsen, and R. R. Alcon. Shock initiation studies of low density HMX using electromagnetic particle velocity and pvdf stress gauges. In *Tenth (International) Symposium on Detonation, Boston, MA*, 1993.

[10] D. S. Stewart, B. W Asay, and K. Prasad. Simplified modeling of transition to detonation in porous energetic materials. *Phys. Fluids*, 6:2515–2534, 1994.

[11] J. W. Nunziato S. L. Passman and E. K. Walsh. A theory of multiphase mixtures. In C. Truesdell, editor, *Rational Thermodynamics*, chapter Appendix 5c, pages 286–325. Springer-Verlag, second edition, 1984.

[12] M. R. Baer and J. W. Nunziato. A two-phase mixture theory for the deflagration-to-detonation transition in reactive granular materials. *Int. J. Multiphase Flow*, 12:861–889, 1986.

[13] P. Barry Butler and Herman Krier. Analysis of deflagration to detonation transition in high-energy solid propellants. *Combstion and Flame*, 63:31–48, 1986.

[14] P. Barry Butler. Ph.d. thesis. Technical report, University of Illinois, Urbana, Illinois, 1984.

[15] S. S. Gokhale and H. Krier. Modeling of unsteady two-phase reactive flow in porous beds of propellant. *Prog. Energy Combust. Sci.*, 8:1–39, 1982.

[16] J. M. Powers, D. S. Stewart, and H. K. Krier. Theory of two-phase detonation-part I: structure. *Combustion and Flame*, 80(3):280–303, 1990.

[17] J. M. Powers, D. S. Stewart, and H. K. Krier. Theory of two-phase detonation-part II: modeling. *Combustion and Flame*, 80(3):264–279, 1990.

[18] A. Bedford and D. S. Drumheller. Recent advances: Theories of immiscible and structured mixtures. *Int. J. Engng. Sci.*, 21:894–897, 1983.

[19] D. A. Drew. Mathematical modeling of two-phase flow. In M. VanDyke, editor, *Ann. Rev. Fluid Mech*, volume 15, pages 261–291. Annual Reviews Inc., 1983.

[20] D. J. Benson. An analysis by direct numerical simulation of the effects of particle morphology on the shock compaction of copper powder. *Modelling Simul. Mater. Sci. Eng.*, 2:535–550, 1994.

[21] P. Embid and M. Baer. Mathematical analysis of a two-phase model for reactive granular materials. *Continuum Mech. Thermodyn.*, 4:279–312, 1992.

[22] E. L. Lee and C. M. Tarver. Phenomenological model of shock initiation in heterogeneous explosives. *Phys. Fluids*, 23:2362–2372, 1980.

[23] R. L. Gustavsen and S. A. Sheffield. Unreacted Hugoniots for porous and liquid explosives. In *High-Pressure Science and Technology - 1993,*

Proceedings of the American Physical Society Topical Group on Shock Compression of Condensed Matter, Colorado Spgs, CO, pages 1393–1396, 1994.

[24] C. Truesdell. Thermodynamics of diffusion. In *Rational Thermodynamics*, chapter 5, pages 219–236. Springer-Verlag, 1984.

[25] M. Renardy and R. C. Rogers. *An Introduction to Partial Differential Equations*. Springer-Verlag, 1996.

[26] A. S. Khan and S. Huang. *Continuum Theory of Plasticity*. John Wiley & Sons, Inc., 1995.

[27] M. M. Carroll and A. C. Holt. Static and dynamic pore-collapse relations for ductile porous materials. *J. Applied Phys.*, 43:1626–1635, 1972.

[28] M. A. Goodman and S. C. Cowin. A continuum theory for granular materials. *Arch. Rational Mech. Anal.*, 44:249–266, 1972.

[29] H. B. Stewart and B. Wendroff. Two-phase flow: Models and methods. *J. Comput. Phys.*, 56:363–409, 1984.

[30] R. J. Atkin and R. E. Craine. Continuum theories of mixtures: Basic theory and historical development. *Quarterly Journal of Mechanics and Applied Mathematics*, 29:209–244, 1976.

[31] R. J. Atkin and R. E. Craine. Continuum theories of mixtures: Applications. *Journal of Mathematics Applications*, 17:153–207, 1976.

[32] H. W. Sandusky, W. L. Elban, and T. P. Liddiard. Compaction of porous beds. In *Shock Waves in Condensed Matter - 1983, Proceedings of the American Physical Society Topical Conference, Santa Fe, NM, July 18-21, 1983*, pages 567–570, 1000 AC Amsterdam, The Netherlands, 1984.

[33] P. J. Coyne, W. L. Elban, and M. A. Chiarito. The strain rate behavior of coarse HMX porous bed compaction. In *Proceedings of Eighth Symposium (International) on Detonation, Albuquerque, NM, July 15–19, 1985*, pages 645–657, White Oak, Silver Spring, Maryland 20903–5000, 1986. Naval Surface Weapons Center.

[34] K. A. Gonthier, R. Menikoff, S. F. Son, and B. W Asay. Modeling energy dissipation induced by quasi-static compaction of granular hmx. In *APS Topical Conference of Shock Compression in Condensed Matter - 1997, Proceedings of the American Physical Society Topical Conference, Amherst, MA*, pages 289–292, 1998.

[35] K. A. Gonthier, R. Menikoff, S. F. Son, and B. W Asay. Modeling compaction-induced energy dissipation of granular hmx. In *Eleventh (International) Symposium on Detonation, Snowmass, CO, Aug. 31, 1998*, 1998.

[36] W. L. Elban and M. A. Chiarito. Quasi-static compaction study of coarse HMX explosive. *Powder Technology*, 46:181–193, 1986.

[37] S. J. P. Palmer and J. E. Field. The deformation and fracture of β-HMX. *Proc. R. Soc. Lond. A*, 383:399–407, 1982.

[38] W. Herrmann. Constitutive equation for the dynamic compaction of ductile porous material. *J. Applied Phys.*, 40:2490–2499, 1969.

[39] M. Carroll and A. C. Holt. Suggested modification of the p–α model for porous materials. *J. Applied Phys.*, 43:759–761, 1972.

[40] D. E. Kooker. Compaction waves in granular material: Numerical predictions. In *JANNAF Propulsion Systems Hazards Meeting, 30 March-3 April, Huntsville, AL, 1987*, pages 7–30, 1987.

[41] T. R. Gibbs and A. Popalato, editors. *LASL Explosive Property Data.* University of California Press, 1980.

[42] A. W. Campbell and J. R. Travis. The shock desensitization of PBX-9404 and composition B-3. In *Proceedings of Eighth Symposium (International) on Detonation, Albuquerque, NM, July 15–19, 1985*, pages 1057–1068, White Oak, Silver Spring, Maryland 20903–5000, 1986. Naval Surface Weapons Center.

[43] P. Embid, J. Hunter, and A. Madja. Simplified asymptotic equations for the transition to detonation in reactive granular materials. *SIAM J. Appl. Math*, 52:1199–1237, 1992.

[44] B. W Asay, S. F. Son, and J. B. Bdzil. An examination of the role of gas permeation during convective burning of granular explosives. *Int. J. Multiphase Flow*, 22:923–952, 1996.

[45] D. ter Haar and H. Wergeland. *Elements of Thermodynamics.* Addison-Wesley, 1966.

[46] S. R. DeGroot and P. Mazur. *Non-equilibrium Thermodynamics.* North-Holland Publishing, Amsterdam–London, 1969.

[47] C. Mader. *Numerical Modeling of Detonation.* University of California Press, 1979.

[48] J. B. Bdzil and S. F. Son. Engineering models of DDT. Technical Report LA-12794-MS, Los Alamos National Lab., 1995.

[49] C. Truesdell. Thermodynamics of homogeneous processes. In *Rational Thermodynamics*, chapter 5, pages 60–81. Springer-Verlag, 1984.

[50] M. R. Baer, R. A. Graham, M. U. Anderson, S. A. Sheffield, and R. L. Gustavson. Experimental and theoretical investigations of shock-induced flow of reactive porous media. In *1996 JANNAF Combustion Subcommittee and Propulsion Systems hazards Subcommittee Joint Meeting (Monterey, CA)*, page 123, 1996.

[51] H-O. Kreiss. *Initial-Boundary Value Problems and the Navier-Stokes Equations.* Academic Press, San Diego, CA, 1989.

[52] D. A. Hills, D. Nowell, and A. Sackfield. *Mechanics of Elastic Contacts.* Butterworth-Heinemann, Oxford, 1993.

Figure Captions and Figures

Figure-1 – Schema showing the forces acting on the HMX grains in a weak compaction wave. The variable gray shaded areas represent the Hertz stresses [52], while the arrows indicate the gas pressure. The unstressed regions of the HMX crystals are shown as light gray. The solid grains "feel" both of these forces.

Figure-2 – The variation in the local number density of grains on the microstructural level appears as a variation of porosity on the continuum level. The variation in porosity acts as a nozzle applied to the gas flow. Darker shading indicates a higher density of particles.

Figure-3 – Quasistatic compression data for porous HMX bed by Elban & Chiarito [36]. Plotted are the fits to their Exps. 8, 9, 11 and 17. Also

shown is the fit to the analytic expression $\beta_s = -\tau \cdot (\phi_s - \phi_s^0) \cdot \ln(\phi_g)/\phi_g$, using $\tau = 1.27 \times 10^{-2}$ GPa and $\phi_s^0 \approx 0.7$.

Figure-4 – The quasistatic compaction curve, $\beta_s = -\tau \cdot (\phi_s - \phi_s^0) \cdot \ln(\phi_g)/\phi_g$ for a granular HMX sample initially at $\phi_s^0 = 0.73$, where $\tau = 12.7\,\mathrm{MPa}$, is shown. Two release isentropes (unloading curves), based on the data in [33] and denoted as $\mathcal{A}$ and $\mathcal{B}$, are also shown. They reveal that the energy recovered from the samples on unloading from $\phi_s = 0.95$ and $\phi_s = 0.85$ is very small (the shaded area). The model treats all the energy under the $\phi_s \beta_s$ curve as being recoverable.

Figure-5 – Hugoniot loci (a) in the P–V plane and (b) in the T_s–P plane. The dotted line is the locus for non-porous (pure) solid. The other three loci are for porous solid with $\phi_s^0 = 0.73$. Whether compaction energy (B-integral) is included in the jump condition has little influence on the pressure. The short dashed line neglects in addition variations in density, *i.e.* $\rho = \phi_s \rho_s^0$.

Figure-6 – The ratio of the compaction work to the B-integral (*i.e.*, $\left[\frac{P_s}{2\rho_s^0}(\frac{\phi_s}{\phi_s^0} - 1) - B\right]/B$) *vs* the inverse of the final state of compaction $(1/\phi_s)$ is shown for two representative cases. The compaction work is roughly 2-3 times the B-integral at $\phi_s = 0.95$. Since only the compaction work measures the dissipated energy in this model, the present model underestimates the total "frictional" heating available for reaction ignition by 25-33% for these examples. Larger errors are made for lower pressure waves.

Figure-7 – The initial reaction rate (computed using the Arrhenius form given above) as a function of shock temperature (see Appendix I). The dotted and solid lines correspond to initial solid volume fraction $\phi_s = 1$ and 0.73, respectively. The effects of porosity are dramatic at higher pressures, leading to a much higher bulk solid temperature and very rapid reaction.

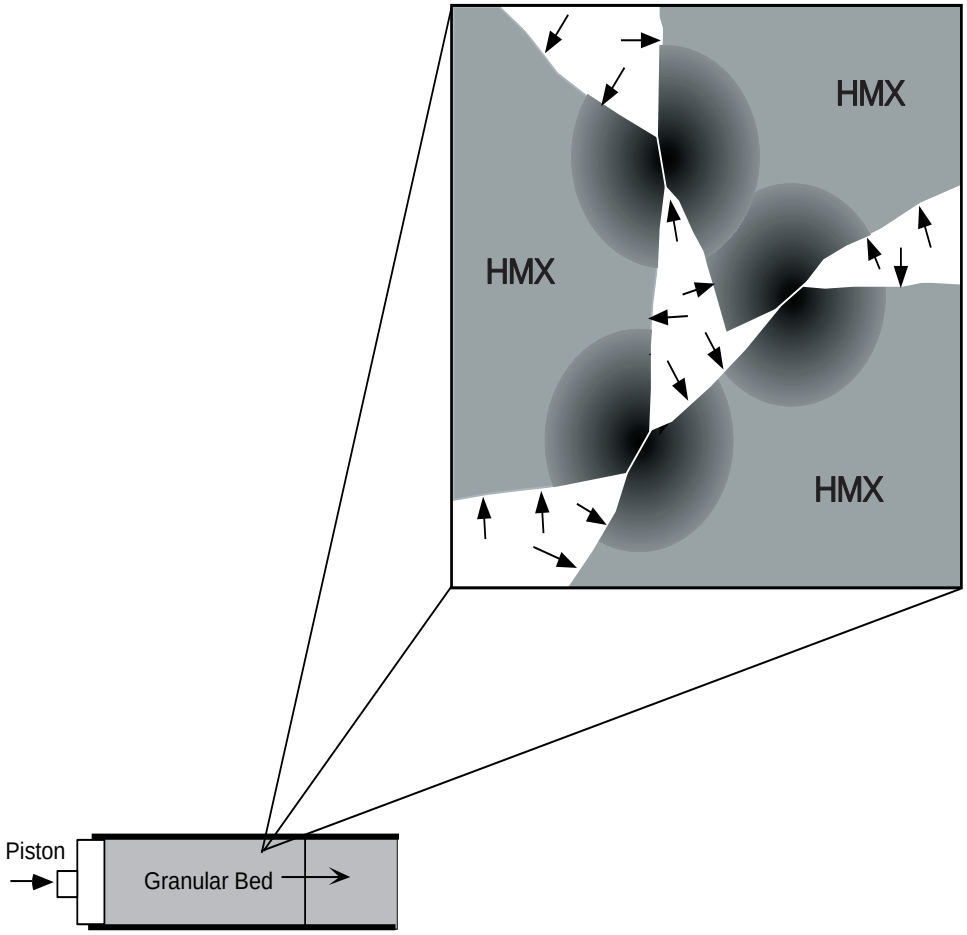

Figure 1. – Bdzil, Physics of Fluids

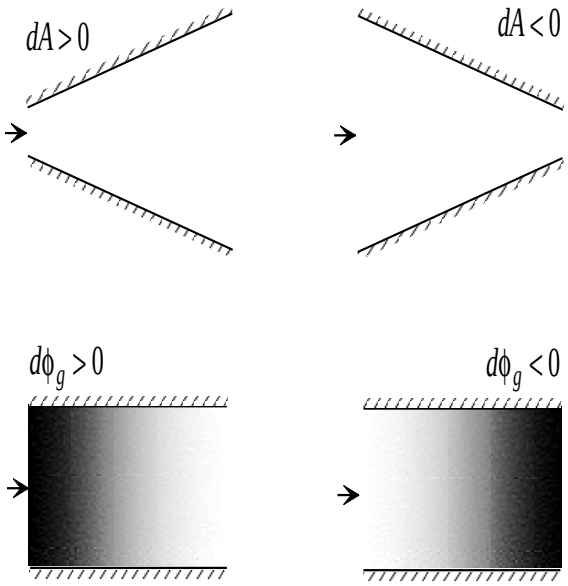

Figure 2. – Bdzil, Physics of Fluids

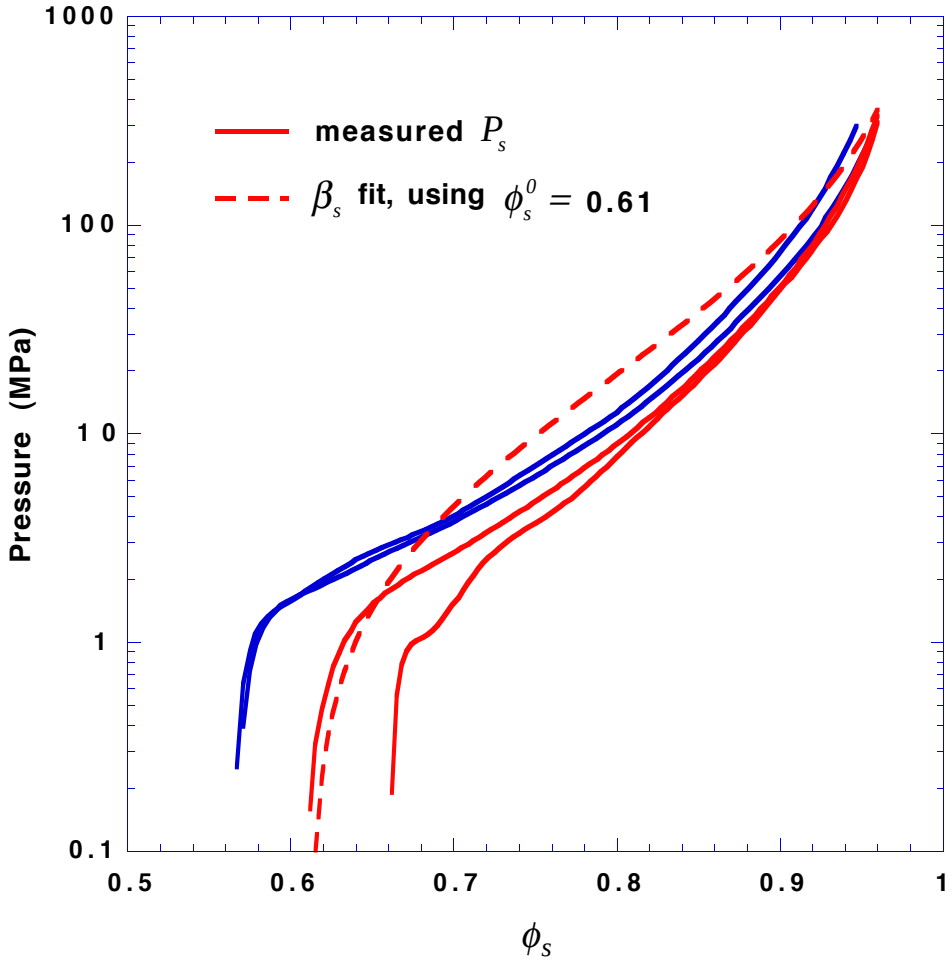

Figure 3. – Bdzil, Physics of Fluids

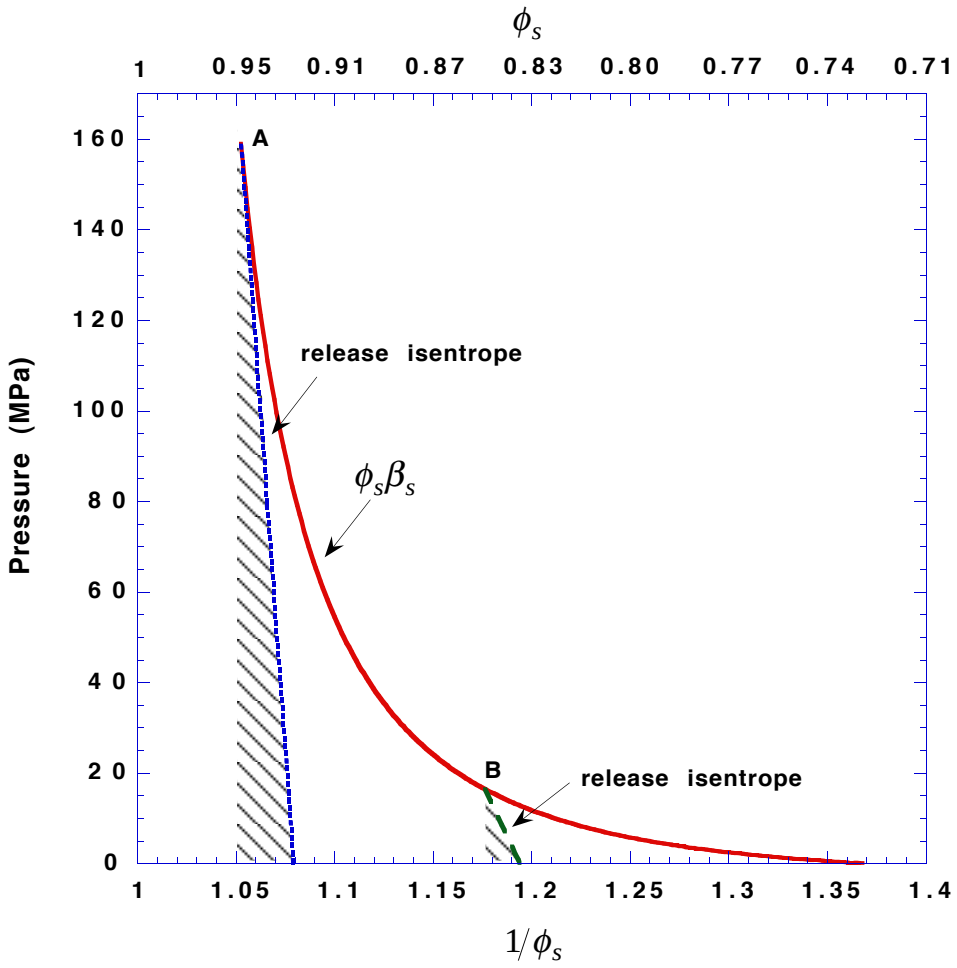

Figure 4. – Bdzil, Physics of Fluids

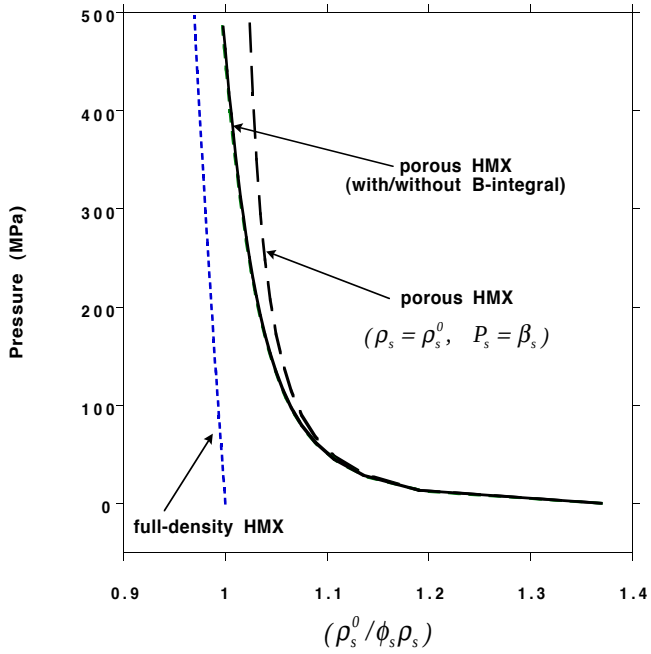

Figure 5a. – Bdzil, Physics of Fluids

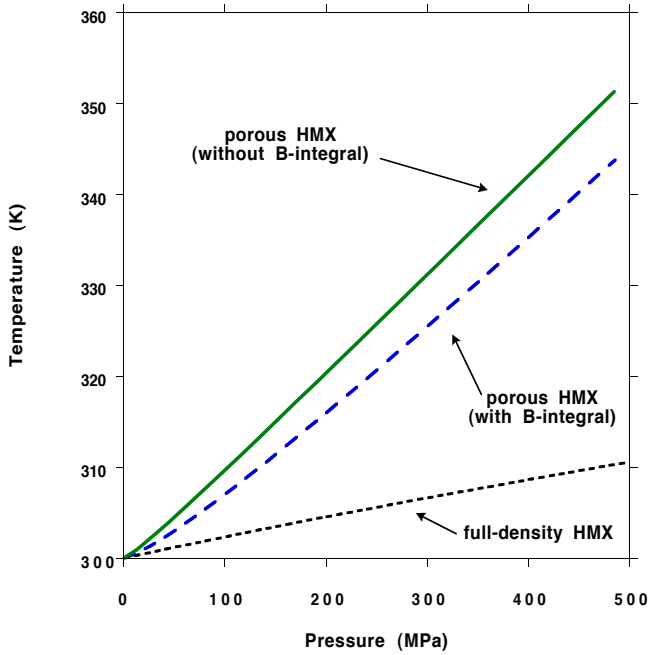

Figure 5b. – Bdzil, Physics of Fluids

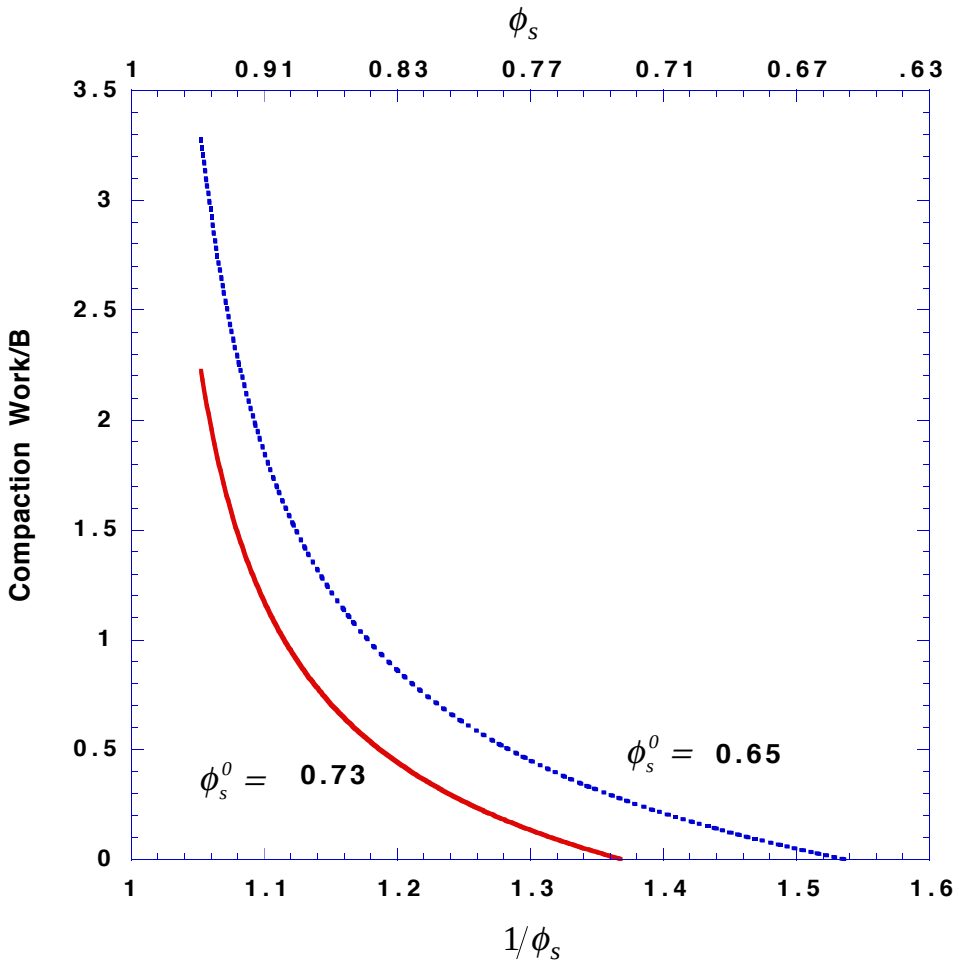

Figure 6. – Bdzil, Physics of Fluids

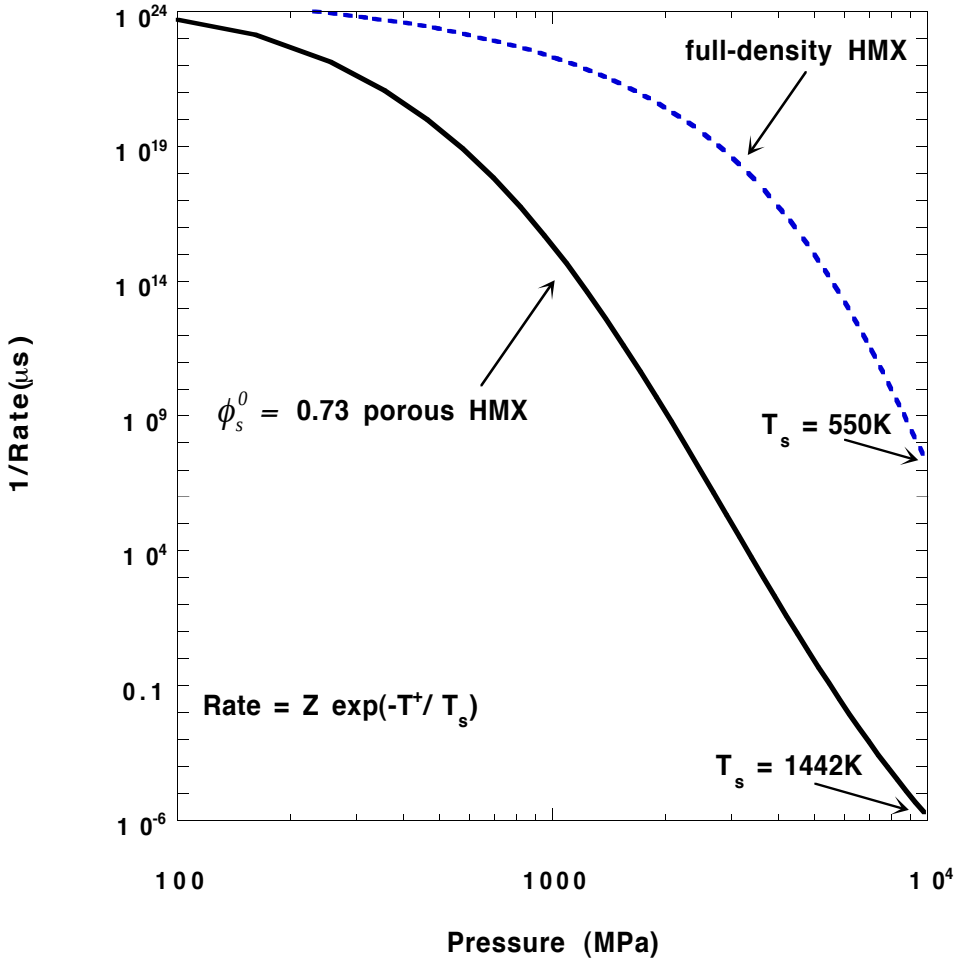

Figure 7. – Bdzil, Physics of Fluids